Trapping synthetic dye molecules using modified lemon grass adsorbent

Mohd Azmier Ahmad[a], Nur'Adilah Ahmed[a], Kayode Adesina Adegoke[b,c], and Olugbenga Solomon Bello[b,d,*]

[a]School of Chemical Engineering, Engineering Campus, Universiti Sains Malaysia, Nibong Tebal, Penang, Malaysia;[b]Department of Pure and Applied Chemistry, Ladoke Akintola University of Technology, Ogbomoso, Oyo State, Nigeria;[c]Department of Chemistry, University of Pretoria, Pretoria, South Africa;[d]Department of Physical Sciences, Industrial Chemistry Programme, Landmark University, Omu-Aran, Nigeria

* CONTACT: Olugbenga Solomon Bello. Department of Pure and Applied Chemistry, Ladoke AkintolaUniversity of Technology, P.M.B 4000, Ogbomoso, Oyo State, Nigeria. Email: osbello06@gmail.com or osbello@lautech.edu.ng

Abstract

Physicochemical method was used to prepare lemongrass leaf activated carbon (LLAC) for removal of Remazol brilliant violet 5 R (RBV5R) dye from aqueous solutions. The surface area, mesopore surface area, total pore volume and average pore diameter of the LLAC are 836.04 m^2/g, 598.6 04 m^2/g, 0.472 04 cm^3/g and 3.62 nm, respectively. The surface functional groups of LLAC before adsorption showed the existence of C–H, O–H, C-O, C = O, C = C, CH_3, N–O and C–N; they are significantly altered after adsorption. The equilibrium data were fitted into Freundlich, Langmuir, Dubinin Radushkevich, Temkin, Koble Corrigan, Vieth Sladek, Radke Prausnitz and Brouers Sotolongo isotherm models. The Koble Corrigan and Freundlich models gave the best fit judging from the correlation coefficient (R2). The monolayer adsorption capacities (qm) obtained for Langmuir and Koble Corrigan isotherm models are 125 and 342.9 mg/g respectively. Kinetic data were fitted using pseudo-first order, pseudo-second order, intraparticle diffusion, Elovich, Boyd and Avrami models respectively. Thermodynamic parameters (ΔS^0, $\Delta H^0$and ΔG^0) were estimated. The mean adsorption energy E_a was 2.811 kJ/mol signifying that the adsorption is physically controlled. This study revealed that lemongrass leaf is effective in removing RBV5R dye from aqueous systems.

Graphical abstract

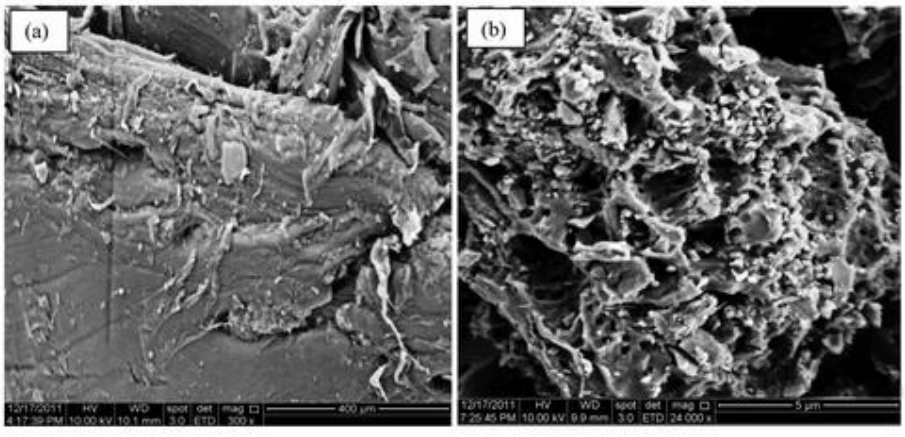

SEM micrographs of (a) lemongrass leaf, char (b) lemongrass leaf, AC

Keywords: Activated carbon; lemongrass; RBV5R dye; adsorption; physisorption; endothermic

Introduction

Industrial effluents are associated with momentous levels of organic and poisonous pollutants which has bad odor and unattractive colors. Dyes are habitually non-degradable by biological method and not effectively removed by conventional physicochemical methods, thus making its removal a serious challenge for textile industries.[1–6] The presence of dyes in the environment is a great threat to both aquatic and human life. Globally, the growth of textile, tanning, leather, paper, plastics, rubber, cosmetics, food industries, etc, to boost the economic status of any nation is amazing in recent years. About 10,000 different types of dyes are produced annually from different industrial processes which weigh approximately one million tons.[1–5] The effluents are released into the environment with no prior or proper treatment resulting to environmental problems affecting both plants and animals. The accumulation of such effluents on yearly basis renders the ecosystem dangerous resulting in killing of aquatic organisms and water contamination thereby making it unfit for drinking and irrigation purposes. The presence of dyes in the receiving bodies; even in minute quantity is carcinogenic and toxic due to their inert nature and non biodegradable abilities.[1–5,7–12]

Numerous technologies are employed for dye treatments, these includes; adsorption, coagulation, flocculation, oxidation, precipitation, electrolysis, reverse osmosis and liquid membrane separation. Despite a notable degree of successes reported for these methods, by comparison, all these methods except adsorption have some inherent restrictions and drawbacks such as high operating cost, generation of extremely hazardous by-products, the energy required is drastically intensive, complexity of the design and operation.[1,8] Among all treatment techniques available, adsorption remains the most superior method for treating wastewater owing to its simplicity of design, ease of operation, re-usability and sensitivity to toxicants.[13] In addition, adsorption is also capable of removing the remaining dissolved pollutants from chemical oxidation and biological treatment. ACs has become known as the only promising alternative to these conventional technologies in dye and wastewater treatment techniques. Adsorption process has been confirmed as one of the most versatile wastewater treatment technologies in the world and it makes use of a wide range of adsorbents.[1–6,14–19] Due to its high efficiency, activated carbon has been used as a promising material in the removal of several dyes.[1–6,10,14–23]

Nowadays, the commonly used adsorbent is activated carbon which is able to remove dyes but the costs of purchasing AC restricted their use in wastewater treatment.[1] The goal of replacing costly commercial AC with agricultural materials has become a promising option owing to their low-cost, availability and efficiency in removing dyes, thus giving the advantage of partly reducing the volume of the wastes and by-products generated in the environment. Additionally, in view of the low cost, regeneration potential and high adsorption capacity, agricultural wastes have been widely employed.[1,16–18] Several methods used to increase the porosity of the adsorbent and the corresponding sites of adsorption have attracted numerous attentions over the past years. Of recent, alternative options of modifying the surfaces of adsorbents for enhanced dye removal from aqueous solution have been investigated; these modifying agents increase the adsorption site(s) for adsorption of both cationic and anionic dyes. Examples of adsorbents materials reported includes: ficus racemosa,[21,24] guava leaf,[25] C. camphora

leaves,[26] plant leaf,[27] bamboo,[28,29] Glossogyne tenuifolia leaves,[30] kola nut,[31,32] bean husk,[31,32] coconut leaf,[33,34] Prunus Dulcis,[35] dead leaves of plane trees,[36] durian seed,[37] Moringa oleifera leaf,[38,39] Prunus dulcis,[35] berry leaves,[40] etc. Literature has demonstrated the peculiarity of agricultural-based materials in the removal of various dyes having diverse molecular structures. Nevertheless, synthesizing and preparing such kinds of functionalized cellulosic adsorbents for efficient dye removal remains a hot topic globally.

Lemongrass leaf, *Cymbopogon citratus* is a genus of about 55 species of grasses, native to warm, temperate and tropical regions of the old world and Oceania. It was introduced to South Asia since precolonial times and to South America, Central America and Madagascar after World War I. *Cymbopogon citratus* is known as *serai dapur*, *sereh* or *serai* in Malaysia and Indonesia. Essential oils are usually extracted from the leaves of *C. citratus*. Once these oils are extracted the remaining leaves are discarded as garbage which accumulates and constitute a nuisance to the environment. Therefore, the application of these wastes as potential carbon sources for preparing AC is at present a fascinating topic due to its availability at zero/low-cost. Placing value on this waste will result in cleaning the environment.[41]

Remazol Brilliant Violet 5 R (RBV5R) dye, an anthraquinone derivative, is a significant anionic dye in the textile industries. RBV5R dye belongs to a class of recalcitrant and toxic organo-pollutants.[1,42–46] They contained chromophoric groups and therefore they are not usually degraded by conventional chemical and physical processes.[2,47,48] Chemical activation was employed in this study. This study aimed at investigating AC derived from lemongrass leaf waste for the removal of RBV5R dye. To the best of our knowledge, for the first time we are reporting the application of AC derived from lemongrass leaf waste as an adsorbent for removing RBV5R dye from aqueous solutions. Adsorption data were tested using eight isotherm models, while the kinetic of the adsorptions were investigated by using six different models. Thermodynamic parameters and the mechanism controlling the interaction were studied.

Materials and methods

Precursor used

Lemongrass leaves (LL) was obtained from Parit Buntar, Perak, Malaysia. All other reagents used in this study are of analytical grades.

Adsorbate

Remazol brilliant violet dye used was supplied by Sigma-Aldrich (M) SDN BDH, Malaysia. A 500 mg/L concentration of RBV5R dye stock solution was prepared by dissolving 0.5 g RBV5R dye powder in 1000 ml deionized water. Serial dilution method was used to prepare different solutions of initial concentrations of 25 mg/L, 50 mg/L, 100 mg/L, 200 mg/L, 400 mg/L and 500 mg/L from the initial stock solution using deionized water. Table 1 presents the physic chemical properties of RBV5R dye.

Table 1. Properties of RBV5R.

Dye name	Remazol Brilliant Violet 5R
Molecular formula	$C_{20}H_{16}N_3Na_3O_{15}S_4$
Molecular weight, g/mol	735.56
CAS no.	12226-38-9
λ max.(nm)	577
Chemical structure	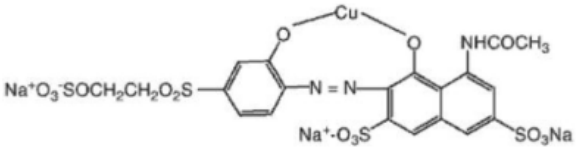

Preparation of adsorbents

Lemongrass leaf (LL) was dried at 378 K for 24 hrs to eliminate its moisture content. The pretreated material was then carbonized at 973.15 K under nitrogen atmosphere for 1 h (first pyrolysis). The certain amount of the char (LLchar) produced were pulverized and then soaked in sodium hydroxide solution (NaOH) at impregnation ratio of 1:1 (NaOH pellets:char) (g/g). The mixture was stirred and dehydrated in the oven at 373.15 K for impregnation over a period of 12 hours. Then, the as-obtained impregnated sample was loaded into a stainless steel vertical tubular reactor and positioned in a tube furnace. The impregnation ratio (IR) was defined as:

$$\mathrm{IR} = \frac{w_{NaOH}}{w_{char}} \qquad [1]$$

where w_{NaOH} and w_{char} are the dry weight of NaOH pellets (g) and char (g) respectively.

Second pyrolysis was carried out at 1073.15 K under N_2 gas flow at 150 cm^3/min. Upon reaching the final temperature, N_2 gas flow was switched to CO_2 at 150 cm^3/min flow rates for the completion of the activation process. The products obtained were cooled to room temperature and later washed in hot deionized water until the pH 6-7 of the solution was attained. Lastly, the sample was dried at 373.15 K and stored in an airtight bottle. The yield was expressed as the dried weight (W_o) of AC per weight of the char (W_c) used for activation.

$$\text{Yield } (\%) = \frac{W_c}{W_0} \times 100 \qquad [2]$$

Adsorbent characterization

Scanning electron microscope (SEM) (Quanta-450FEG, Netherland) was used to examine the surface morphologies of LLchar and LLAC. This provides information on both qualitative and quantitative particle morphologies and surface appearances of the adsorbents which were analyzed by ranges of detectors to form a 3D image. Simultaneous thermal analyzer (PerkinElmer STA6000, USA) was used to study the proximate analysis of the sample. This was done to determine the fixed carbon, moisture contents, volatile matter, and ash contents that are present in the samples as described in our previous studies.[38,49] For the determination of the volatile matter, the temperature was raised to 850 °C and held for 7 minutes and subsequently decreased to 800 °C. Then, the N_2 gas was switched to O_2 gas to create an oxidizing atmosphere for fixed carbon content determination. The remaining masses after this analysis constituted the ash contents. Elemental analysis was done via an elemental analyzer, (PerkinElmer 2400SeriesII, USA).

Surface functional groups were investigated using an FTIR spectrophotometer (Shimadzu model IRPrestige-21). The spectroscopic investigation enables the study of the surface chemistries of LLAC before and after adsorption. The spectra reveal the characteristics' details of the functional groups present in LLAC before and after adsorption. The samples are encapsulated in the potassium bromide pellet. They are measured from 4000 to 400 cm^{-1}. The analysis is done automatically by software which attached to the system (Spectrum version 5.0.2). The pore volume, average pore diameter, and surface area were determined using Micromeritics ASAP2020 volumetric adsorption analyzer while the Brunauer-Emmett-Teller (BET) was used to measure the surface area of the adsorbent. The total pore volume was determined in liquid N_2 volume at 0.98 relative pressure.[50]

Batch sorption experiments

Batch adsorption studies were carried out at 25 °C, 45 °C and 60 °C. Six different concentrations (25 mg/L, 50 mg/L, 100 mg/L, 200 mg/L, 400 mg/L and 500 mg/L) were prepared in Erlenmeyer flasks. To each concentration, 0.10 g LLAC was added to each flask filled with a 100 ml RBV5R dye solution. The flasks were closed and positioned in an isothermal water-bath shaker at 30 °C constant temperature and a speed of 80 rpm until equilibrium is attained. The aqueous samples were withdrawn at a fixed time interval to measure the concentrations using a UV/Vis spectrophotometer at 520 nm wavelength. The same procedure was applied at solution temperatures of 45 °C and 60 °C. For kinetic and equilibrium investigations, dye uptake at time t (i.e., q_t (mg/g)) and equilibrium, q_e (mg/g)), are calculated using Eqs. (1) and (2). Eq. (3) was employed to calculate the percentage removal at equilibrium.

$$q_t = \frac{(C_o - C_t)V}{W} \quad [1]$$

$$q_e = \frac{(C_o - C_e)V}{W} \quad [2]$$

$$\text{Percentage of dye removal } (\%) = \frac{(C_e - C_t)}{C_t} \text{ x } 100 \quad [3]$$

where C_t, C_o, and C_e (mg/L) are liquid-phase concentrations of RBV5R dye at time, t, initial solute concentration, and liquid-phase concentrations of RBV5R dye at equilibrium respectively. V is the volume of the solution (L) and W is the mass of adsorbent (g).[10,51]

Validity of adsorption isotherm

In order to validate the isotherm that best describes the experimental data, the normalized standard deviations (Δqe (%)) were employed (Eq (4)) to support the correlation regression (R^2) value which is common to all models.

$$\Delta q_e \left(\%\right) = 100 \times \sqrt{\frac{\sum_i^n \left[\left(q_{e,\exp} - q_{e,cal}\right)/q_{e,\exp}\right]^2}{n-1}} \quad [4]$$

where n is the number of the data point, $q_{e.exp}$ and $q_{e.cal}$ (mg/g) is the experimental and calculated equilibrium adsorption capacities respectively. This parameter measures the difference

between the amounts of adsorbed RBV5R dye predicted by the models and experimental values: the lower the value of Δq_e, the better the fit.[52,53]

Kinetic and isothermal studies

Adsorption kinetic provides reaction mechanisms and pathways, relating the rates of adsorption with the concentrations of adsorbate in solution. Adsorption kinetic for removal of RBV5R dye by LLAC was investigated using pseudo first order (PFO), pseudo second order (PSO), Elovich, Avrami, Boyd and intraparticle diffusion (IPD) models respectively. The adsorbate and adsorbent interactions were analyzed via seven isotherm models: Langmuir, Freundlich, Temkin, Dubinin Radushkevich (DR), Koble Corrigan (KC), Vieth Sladek (VS), Radke Prausnitz (RP) and Brouers Sotolongo (BS) isotherm models. Table 2 presents the kinetic and isotherm parameters for RBV5R dye adsorption onto LLAC.

Table 2. Adsorption isotherm and kinetics parameters.

Adsorption model	Type	Equation		Expression of the equation	Ref.
Isotherm	Langmuir	$\frac{C_e}{q_e} = \frac{1}{q_m C_e} + \frac{1}{K_L q_m}$ $R_L = \left[\frac{1}{(1 + K_L Co)}\right]$	(5) (6)	C_e is the adsorbate concentration at equilibrium (mg/L), q_e is the amount of adsorbate adsorbed per unit mass of adsorbent (mg.g^{-1}), q_m is the maximum monolayer adsorption capacity of the adsorbent (mg.g^{-1}), K_L; the Langmuir adsorption constant (L.mg^{-1}). C_o is the highest initial solute concentration; whereas, R_L value implies the adsorption is unfavorable {($R_L > 1$), linear ($R_L = 1$), favorable ($0 < R_L < 1$), or irreversible ($R_L = 0$)}.	[54]
	Freundlich	$\ln q_e = \frac{1}{n} \ln C_e + \ln K_f$	(7)	K_f is the Freundlich isotherm constant ((mg.g^{-1}) (L.mg^{-1})); n, the heterogeneity factor. The slope of 1/n ranging between 0 and 1 is a measure of adsorption intensity, which becomes more heterogeneous as the values get closer to zero.	[55]
	Temkin	$q_e = B \ln K_T + B \ln C_e$	(8)	$B = R_T/b$ is the constant related to the heat of adsorption (L.mg^{-1}); T is absolute temperature; R is universal gas constant (8.314 J/mol K); K_T, equilibrium binding constant (L.mg^{-1}).	[56]
	D–R	$\ln q_e = \ln q_m + \beta \varepsilon^2$ $\varepsilon = RT \left[1 + \frac{1}{C_e}\right]$ $E = \frac{1}{\sqrt{2\beta}}$	(9) (10) (11)	β a constant related to the adsorption energy (mol^2/kJ^2); ε is the Polanyi potential, E is adsorption energy (when value of E is between 1 and 8 kJ/mol, it implies a physical adsorption while value between 9 and 16 kJ/mol means a chemical adsorption.	[25,57,58]
Kinetics	PFO	$\ln(q_e - q_t) = \ln q_e - K_1$	(12)	$q_t$is the amount of solute adsorb per unit weight of adsorbent at time t (mgg^{-1}), K_1 is the pseudo-first order kinetics rate constant (min^{-1}).	[59]
	PSO	$\frac{t}{q_e} = \frac{1}{K_2 q_e^2} + \frac{1}{q_e} t$	(13)	K_2 is pseudo-second order kinetics rate constant (min^{-1}).	[60]
	Elovich	$q_t = \frac{1}{\beta} \ln(\alpha\beta) + \frac{1}{\beta} \ln t$	(14)	α is the initial desorption rate [mg. (g min)$^{-1}$], β, the desorption constant (g.mg^{-1}). The 1/b value denotes the number of available sites for adsorption and the value of (1/ β); (ln $\alpha\beta$) shows quantity of adsorption when (ln t) equal to zero.	[61,62]
	IPD	$q_t + K_{diff} t^{1/2} + C$	(15)	C is the intercept and reflects the boundary layer effect of the plot $q_t$against $t^{1/2}$. K_t(mg/g h$^{1/2}$) denotes the intra-particle diffusion rate constant; t$^{1/2}$, the half-adsorption time (h$^{1/2}$). For intra-particle diffusion to be the only rate determining step, then the regression of $q_t$against t$^{1/2}$ must be linear and should pass through the origin, otherwise, it then implies that the intra-particle diffusion is not the only rate-controlling step	[63,25,39]

Adsorption thermodynamic studies

Gibbs free energy (ΔG˚), enthalpy change (ΔH˚) and entropy change (ΔS˚) described in Eqs. (23)–(25) were used to explain the thermodynamics of RBV5R dye adsorption onto LLAC at three different temperatures (303, 313 and 323 K):

$$\Delta G^{\circ} = -RT\ lnK_L \quad [23]$$

$$\ln\ K_L = \frac{\Delta S^{\circ}}{R} - \frac{\Delta H^{\circ}}{RT} \quad [24]$$

The ΔS and ΔH values are the intercept and slope of the Van't Hoff plot of ln K_L vs 1/T. K_L value is the Langmuir constant (L/mol) determined from the lnq_e/C_e relation at 303 K, 313 K, and 323 K. Energy of adsorption (i.e., the minimum energy required by the reactants for interaction (s) to proceed) was calculated using the Arrhenius equation (Eq. (25)):

$$\Delta G^{\circ} = -RT\ lnK_L \quad [25]$$

where K_2 is the PSO rate constant (g. (mg h)$^{-1}$), E_a(kJmol^{-1}) is the Arrhenius energy of activation of RBV5R dye adsorption, A is the Arrhenius factor, R is the universal gas constant. The plot of ln K_2 against 1/T gives a straight-line graph with a slope of $-E_a/R$.

Results and discussions

Characterization of lemongrass leaf AC (LLAC)

Proximate analysis

Lemongrass leaf used in this study was rich in the volatile matter and moisture contents which become drastically decreased from LL raw to LLAC samples. This significant decrease was as a result of activation and carbonization process at higher temperature; this affected the stability of organic compounds leading to breakage and linkage of bonds as a result of heat. During this process, volatile matters are released as liquid and gaseous products finally evaporated leaving only materials of high carbon contents.[48,50,64,65] This implies that activation at higher temperature broke down the lignocellulosic materials followed by the volatilization of the volatile compounds,[31,66] leading to an increased reaction rate during C-NaOH activation process. This of course results in "carbon burn off," which resulted in the development of better porous surface on the LLAC samples. Proximate analyses show that physiochemical activations successfully improved the fixed carbon contents and reduce the volatile matter (Table 3). The LLAC sample revealed relatively low moisture content, volatile matter and ash content; this implies that LLACs are good adsorbent materials for RBV5R dye removal. The lower ash contents obtained for the LLAC as shown in Table 3indicates its suitability as a good adsorbent. It should be noted that high ash content decrease the effectiveness and performance of AC, meaning that the lower the adsorbent ash contents, the better its performance and efficiency for dye removal.[38,67]

Table 3. ***Proximate content of precursor, char and activated carbon.***

	Proximate analysis (%)			
Sample	Moisture	Volatile	Fixed Carbon	Ash
LLraw	8.80	67.94	18.59	4.67
LLchar	5.13	32.86	57.51	4.50
LLAC	2.93	15.80	77.41	3.86

Surface area and pore size of LLAC

Surface area and pore size are significant features influencing the superiority of adsorbent materials. The BET surface area, mesopore surface area, total pore volume and average pore diameter of the LLAC are 836.04 m^2/g, 598.6 04 m^2/g, 0.472 04 cm^3/g and 3.62 nm, respectively as shown in the Table 4. The process of LL activation with NaOH and CO_2 gasification helped the formation of mesopores which resulted in the formation of LLAC with higher surface area in contrast to the LLchar with lower surface area. The average pore diameter of 3.62 nm implies that LLAC was in mesopore regions with high affinity for RBV5R dye removal.

Table 4. Surface area and pore characteristics of the prepared activated carbons**.**

Sample	BET surface area (m^2/g)	Mesopore surface area (m^2/g)	Total pore volume (cm^3/g)	Average pore diameter (nm)
LLchar	152.44	71.87	0.138	3.47
LLAC	836.04	598.60	0.472	3.62

Surface morphology of LLchar and LLAC

Figure 1a and b shows the corresponding SEM images of LLchar and LLAC. It is obvious that the surface of LLchar (Figure 1a) was uneven and rough, the pores are not well developed. However, Figure 1b reveals the formation of numerous and distinct pores on the LLAC surface. This suggests that one of the significant contributions of the activation process was to widen and open up the pores on LLAC surface, in so doing, the ability for removing RBV5R dye becomes enhanced.[2,38,50] This means that NaOH was efficient in the creation of numerous well- and properly developed pores on the surface of the precursor thereby enhancing the process of adsorption. This was as a result of the large porous structure and surface area of the LLAC.[12,25,65,68]

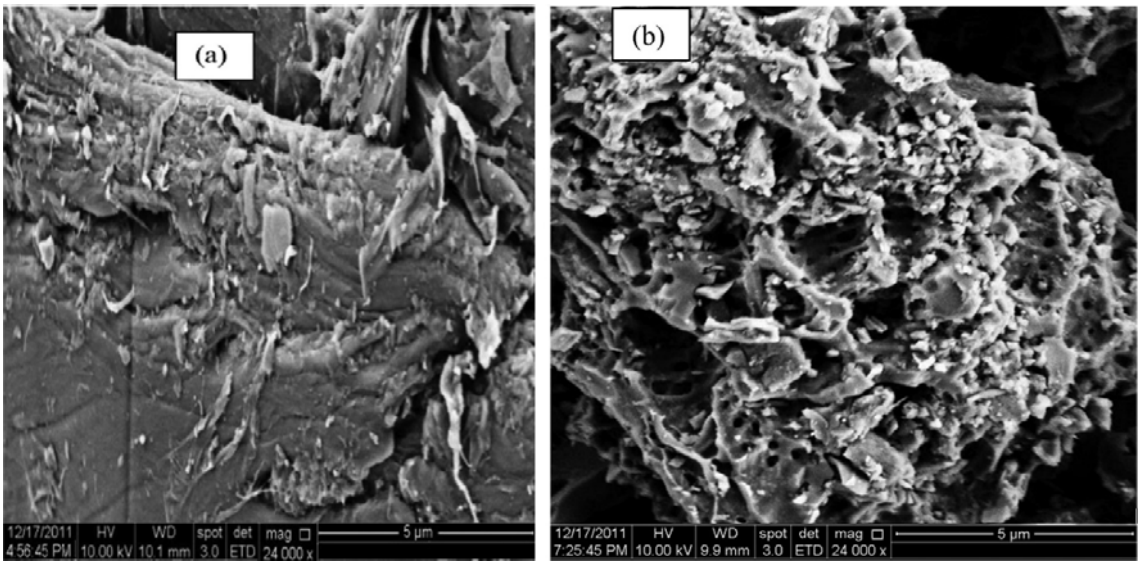

Figure 1. SEM micrographs of (a) lemongrass leaf char (Magnification = 24kx); (b) AC (Magnification = 24k x).

Surface chemistry of LLAC

The porosity as well as the presence of prominent functional groups on the adsorbent surface affect the adsorption capacity.[69] The infrared spectroscopy technique was used for the identification of the functional groups present in the LLAC that are responsible for binding RBV5R dye molecules, and also to elucidate the dye–adsorbent interactions. FTIR spectra of LLAC before and after adsorption of RBV5R dye are presented in Figure 2. For LLAC before adsorption (Figure 2a), the bands at 3571–3200 cm^{-1} assigned to O–H stretch, H-bonding, 2980–2960 cm^{-1} attributed to C–H stretching of alkane, 1737–1708 cm^{-1} attributed to C = O stretch, 1675–1600 cm^{-1} assigned to Aliphatic C = C stretch, 1600–1500 cm^{-1} attributed to N–O asymmetry stretch, 1470–1430 cm^{-1} assigned to C–H bending, 1385–1380 cm^{-1} assigned to CH_3, 1340–1250 cm^{-1} assigned to C–N stretch, 1050 cm^{-1} ascribed to C–O stretch, 1350–1260 cm^{-1} assigned to O–H bending from a carboxylic acid. It was observed that most of the functional groups were greatly altered after adsorption of RBV5R dye (Figure 3b). Comparing both spectra, the disappearance of the following bands 2125 cm^{-1}, 1650.09 cm^{-1}, 1514.46 cm^{-1}, 1386–1273 cm^{-1}, 904–803 cm^{-1} present in LLAC before adsorption were observed (Figure 2a); provides rich chemistry that led to the effective removal of RBV5R dye; as these pores and active sites are opened (Figure 2a), it became occupied by the RBV5R dye molecules after adsorption (Figure 2b). This led to decrease or disappearance in bands and shifting to lower wavelengths (Figure 2b) which suggests the involvement of these functional groups in the binding of RBV5R dye to LLAC.[2,53,70] The change in peak wave numbers confirms the adsorption of RBV5R dye onto the surface of LLAC. This further indicated the involvement of these functional groups in the adsorption of RBV5R dye molecules on the surface of the LLAC through weak electrostatic interaction or Van der Waal forces. This can be considered as further evidence for the interaction between LLAC and the RBV5R dye molecules.[49]

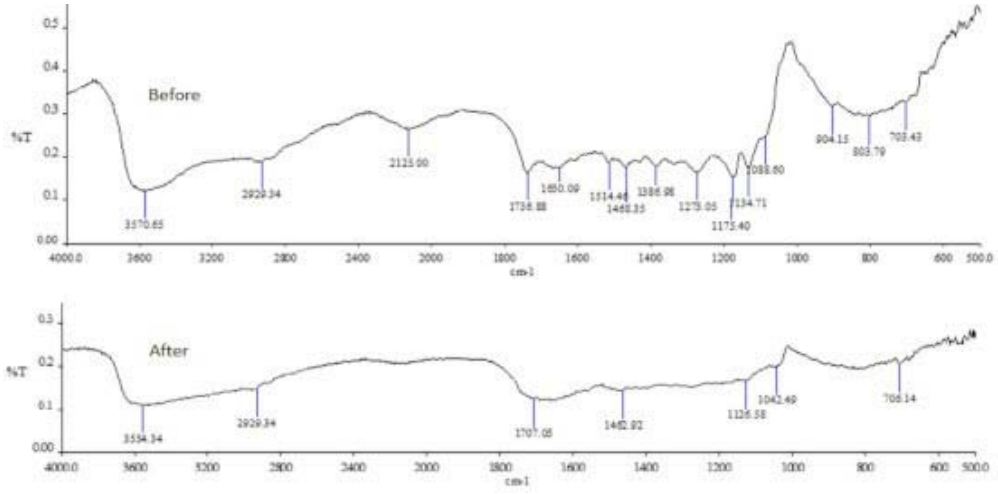

Figure 2. FT-IR of LLAC; (a) before adsorption (b) after adsorption.

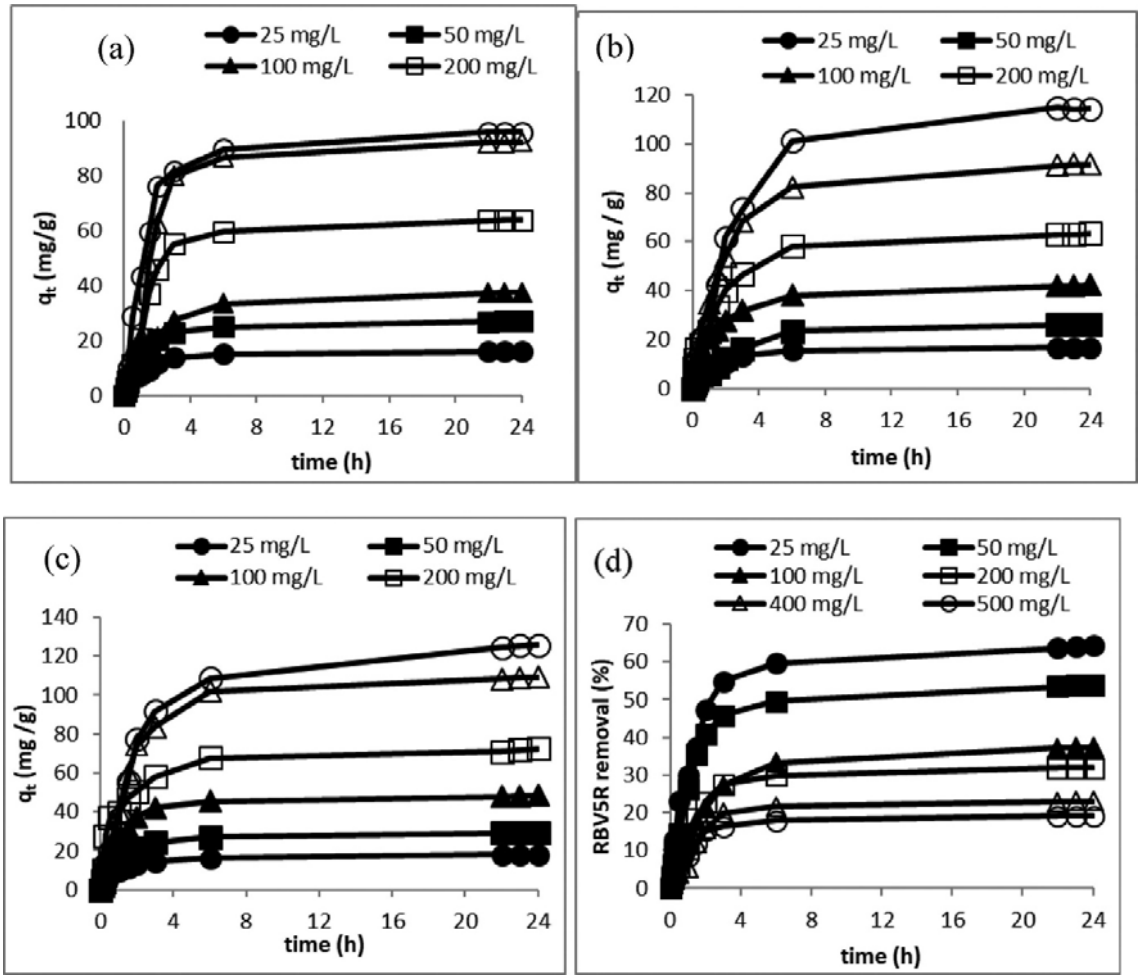

Figure 3. Dye adsorption at different initial concentrations and contact time of RBV5R onto LLAC at (a) 30 °C, (b) 45 °C, (c) 60 °C and (d) RBV5R percentage dye removal at 30 °C.

Batch adsorption studies of RBV5R dye adsorption onto LLAC

Effects of contact time and initial RBV5R dye concentration

The effects of contact time and initial RBV5R dye concentration onto the LLAC at 30 °C, 50 °C and 60 °C are shown in Figure 3a–c. Figure 3d represents the percentage RBV5R dye adsorbed onto the LLAC at different contact times at 30 °C. Plots for adsorption of RBV5R dye onto the LLAC at 45 °C and 60 °C are given in S1 (Supporting information). These results showed that the adsorption of RBV5R dye increases with time. Rapid RBV5R dye uptake was observed at the initial stage of contact periods around 0–6 hours but after 6 hours a very slower dye uptake was noticed until it reaches equilibrium before 24 hours. This was attributed to the availability or accessibility of a large number of vacant sites for adsorption of RBV5R dye at the initial stage.[71] After a lapse of time, the adsorption became slower as a result of the decreased number of vacant sites since these surface sites were almost fully occupied by dye molecules.

In dye adsorption processes, the dye molecules need to first encounter the boundary layer effects first prior to a diffusion onto the adsorbent's surface, thereafter, it diffuses into the adsorbent's porous structures.[72] In fact, at higher initial dye concentrations, the higher RBV5R

dye uptake was obtained as the amount of dye molecules contending for the available sites on LLAC surface are higher. Table 5 presents the adsorption uptake and percentage removal at equilibrium showing that the process of adsorption is highly dependent on the initial RBV5R dye concentrations.

Table 5. Adsorption of RBV5R dyes uptakes and Percentage of dyes removal at equilibrium.

Concentration (mg/L)	Dyes uptake (mg/g)	Dye removal (%)
25	16.11	64.43
50	26.90	53.80
100	37.37	37.37
200	63.73	31.86
400	91.98	23.00
500	95.7	19.14

Effect of solution temperature

Figure 4 revealed the RBV5R dye uptake onto LLAC, q_e (mg/g) obtained at different initial dye concentrations as a function of solution temperature. The amounts of RBV5R dye uptake improved with increase in solution temperature (30–60 °C) at all initial RBV5R dye concentrations. This indicates that adsorption of RBV5R dye onto LLAC is an endothermic process. Increasing the solution temperature results in significant increase in chemical interaction of RBV5R dye with the LLAC surface functional groups. This pave way for increase RBV5R dye mobility to deeply penetrate the LLAC active sites.[48] This, therefore, enhanced the reduction of viscosity of the RBV5R dye solution, showing that the diffusion rate of the RBV5R dye molecule across the external boundary layer and through the internal pores of the LLAC significantly increased. This result is in close agreement with previous studies.[2,49,50,73]

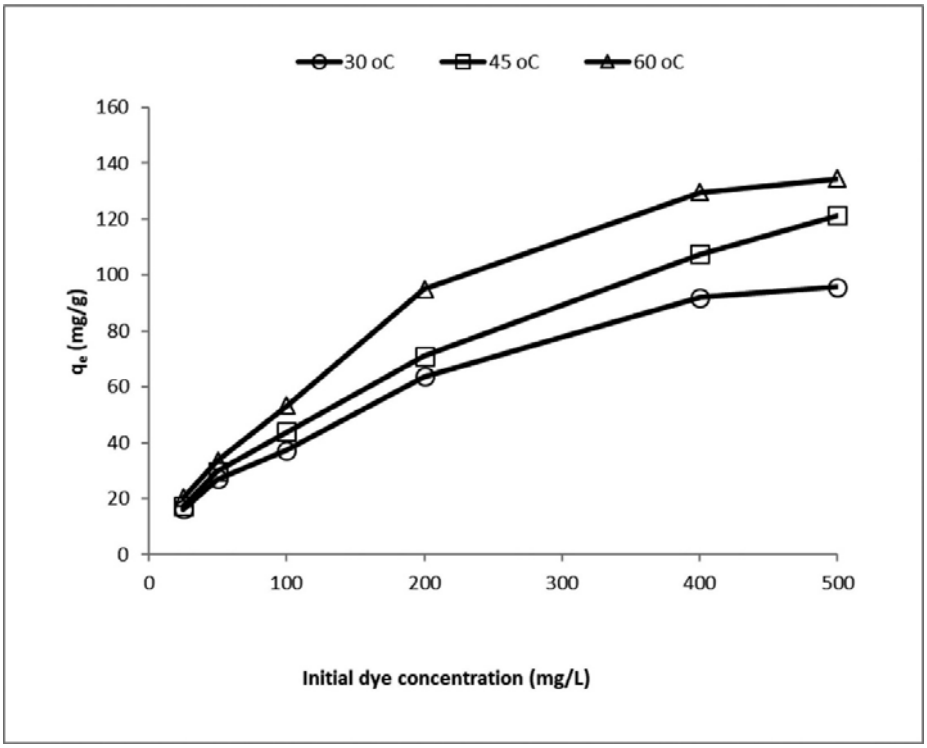

Figure 4. Adsorption of RBV5R dye at different solution temperatures.

Influence of solution pH

Adsorption of organic species is significantly influenced by the solution pH because pH governs the properties of adsorbent and adsorbate molecules such as the surface charge of the adsorbent and ionization degree of the adsorbate molecule.[74–76] The effect of pH on RBV5R dye uptake by LLAC were investigated at pH range of 2.0–12. The percentage dye removal by LLAC was carried out at the following experimental conditions: dose of LLAC (0.1 g), RBV5R dye concentration (100 mg/L), and solution temperature (30 °C). Figure 5 shows the influence of solution pH on the RBV5R dye adsorption. The highest percentage removal was 45.54% for RBV5R dye at the initial dye concentration of 100 mg/L. It shows that the adsorption capacity of RBV5R dye onto LLAC decreased as solution pH increased, at pH 2, the LLAC had the maximum percentage removal at initial RBV5R dye concentration of 100 mg/L. It was observed here that RBV5R dye removal onto LLAC is strongly dependent on solution pH. This is in agreement with previous studies.[74,77] Dissolving RBV5R dye in aqueous media led to the existence of sulfonate groups (Dye-SO_3Na) which become dissociated and converted to anionic dye ions (Dye-SO_3^-). This leads to strong electrostatic interactions involving the RBV5R dye ions and LLAC.[74] In fact, changing the solution pH from 2 to 8 decreases the adsorption capacity further to 36% (Figure 5). The decrease in adsorption capacity when the pH became greater than 2 can be ascribed to the reduction of the positively charged ions on LLAC surface in alkaline medium and also the competition for adsorption on the LLAC active sites between the RBV5R dye ion and hydroxyl ion with increasing solution pH.[74,75,78] This implies that as the initial pH of the system increases, the surface of LLAC becomes more negatively charged, thereby establishing the electrostatic interaction between LLAC surface and RBV5R dye molecules.[78] This electrostatic attraction between the charged surface and charged dye molecule may be considered as the principal adsorption mechanism.[74]

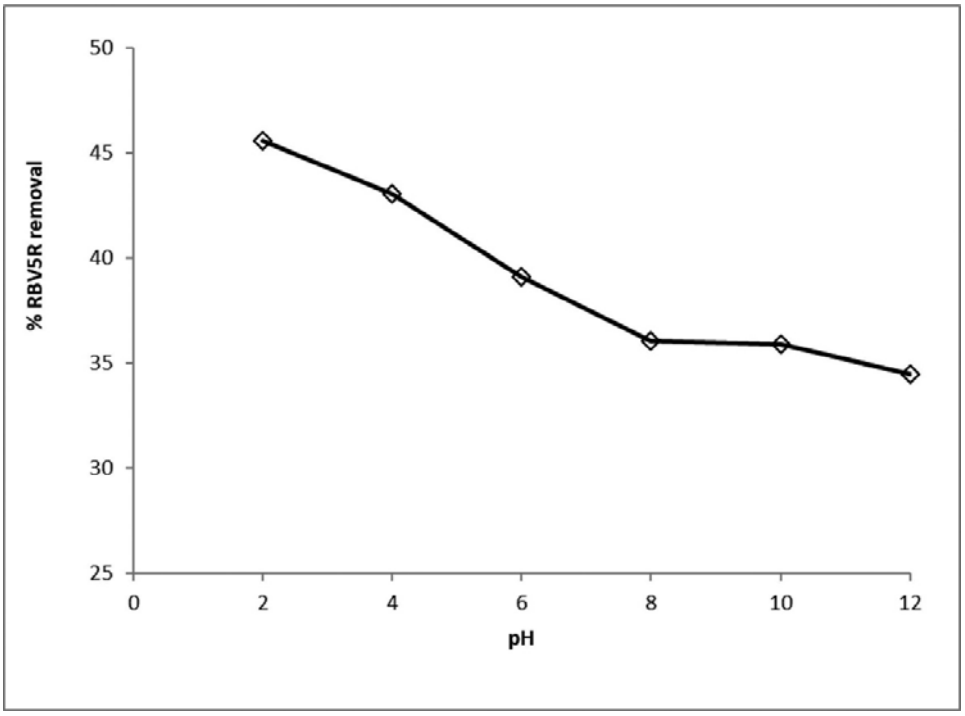

Figure 5. Effect of initial pH on RBV5R dye removal.

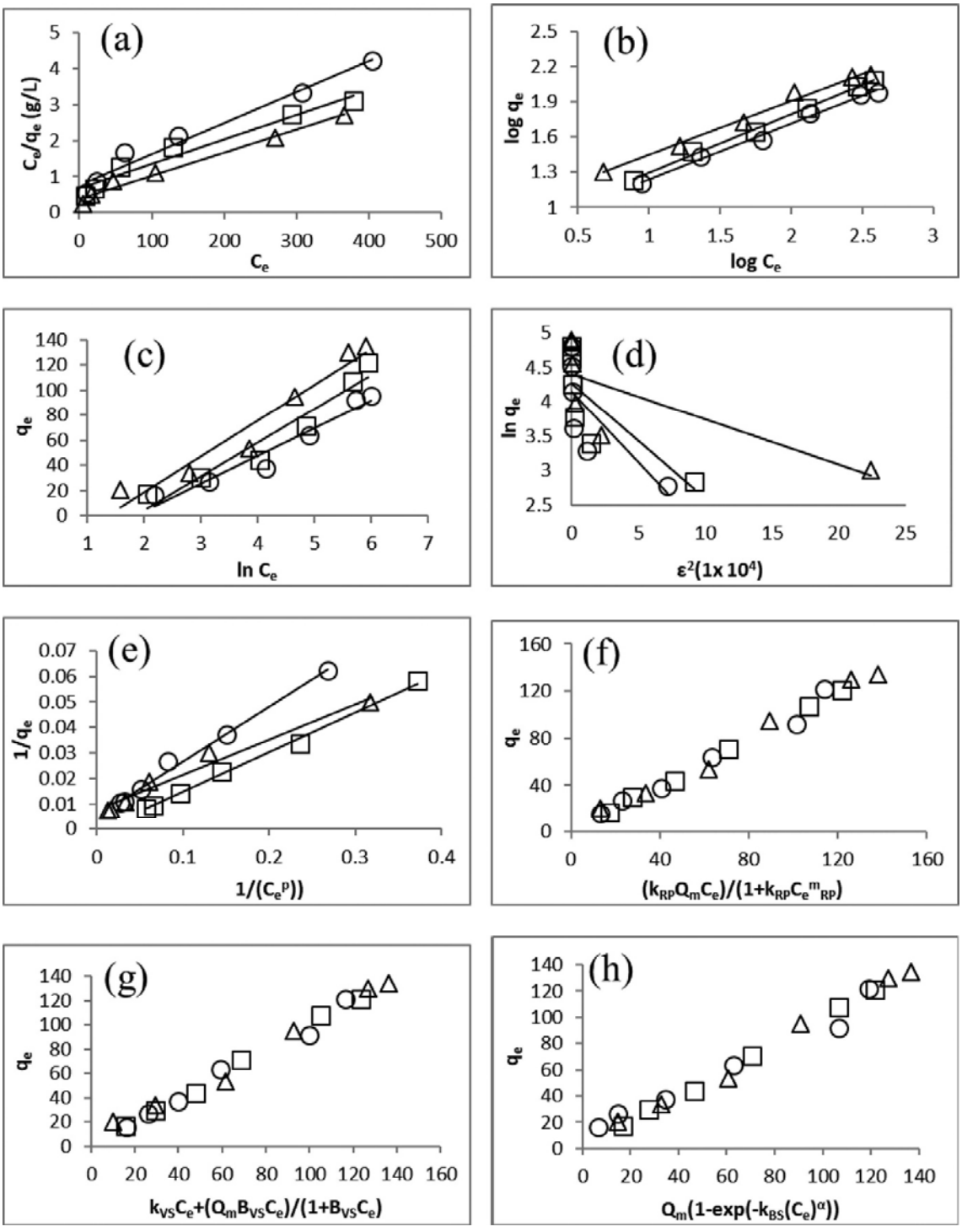

Figure 6. Plot of (a) Langmuir, (b) Freundlich, (c) Temkin and (d) Dubinin-Radushkevich, (e) Koble-Corrigan, (f) Radke-Prausnitz, (g) Vieth-Sladek and (h) Brouers-Sotolongo isotherm for RBV5R adsorption on LLAC at 30°C (^), 45°C (□) and 60°C (Δ).

Adsorption isothermal studies

Adsorption isotherms are employed to explain solute interactions with LLAC when the process of adsorption reaches an equilibrium state. In this study, eight isothermal models were selected for the fitting of the equilibrium data (Figure 6): (a) Langmuir, (b) Freundlich, (c) Temkin, (d) DR, (e) KC, (f) VS, (g) RP and (h) BS isotherm models. These models were used to find the most suitable model(s) that best explained the experimental data. By determining the value of the correlation coefficient, R^2 for all isotherm equations, it is expected that the most suitable model(s) would give the highest R^2 value. The results of the isotherm parameters are presented in Table 6. According to Figure 7, which illustrates the plot of the separation factor (R_L) against the initial RBV5R dye concentration at 30 °C in the concentration range studied (25–500 mg/L), the R_L ranged from 0.245 to 0.795. These values are below 1. This implies a favorable RBV5R dye adsorption onto LLAC, suggesting that the process of adsorption was favored at higher initial RBV5R dye concentrations. The plots obtained for similar adsorption process at 45 °C and 60 °C are also investigated and reported (Figure S2) (supporting information). For the Freundlich isotherm, the value of n_F equal to 2.101, suggesting a favorable physical process. As for the Temkin isotherm, the B constant was 21.99 which indicated an exothermic adsorption reaction.[79] The Vieth–Sladek (VS) (Figure 6g) isotherm best explained the adsorption equilibrium of the RBV5R dye onto LLAC. The VS isotherm is usually employed for estimation of the rate of diffusion in a solid material on transient adsorption. Particularly, it is applicable to the solute that is adsorbed in regard to a definite isotherm: explained by linear components (Henry's law) and nonlinear components (Langmuir eqn). The linear component corresponds to a physical to gas-dissolve amorphous regions, while the nonlinear connotes the adherence of gas molecules to the surface pores on the adsorbent.[80]

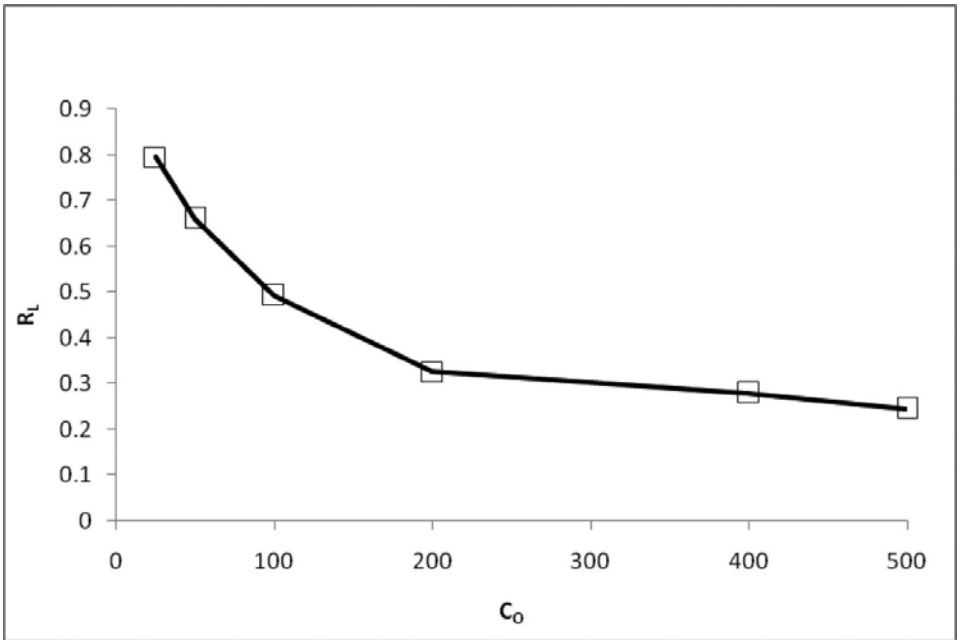

Figure 7. Plot of separation factor versus initial dye concentrations at 30 ^{0}C.

Table 6. Isotherm parameters for RBV5R.

Langmuir	Freundlich	Temkin	Dubinin-Radushkevich	Koble-Corrigan	Radke-Prausnitz	Vieth-Sladek	Brouers-Sotolongo
$q_m = 125.0$	$k_F = 5.728$	$B = 21.99$	$q_s = 63.78$	$A_{kc} = 4.69$	$q_m = 3.781$	$k_{VS} = 0.233$	$q_m = 184.0$
$k_L = 1.03 \times 10^{-2}$	$1/n_F = 0.48$	$A = 0.159$	$E = 158.11$	$B_{kc} = 2.53 \times 10^{-2}$	$k_{RP} = 16631.6$	$q_m = 29.01$	$k_{BS} = 0.005$
			$b_{DR} = 2 \times 10^{-5}$	$n = 0.6$	$m_{RP} = 0.426$	$B_{VS} = 0.109$	$\alpha = 0.9$
				$q_m = 342.9$			
$R^2 = 0.972$	$R^2 = 0.992$	$R^2 = 0.944$	$R^2 = 0.59$	$R^2 = 0.992$	$R^2 = 0.979$	$R^2 = 0.986$	$R^2 = 0.976$

Thus, by comparing the experimental results and isotherm models used, Freundlich and Koble Corrigan models were found suitable for RBV5R dye adsorption (each having $R^2 = 0.992$). Freundlich isotherm model is based on adsorption on the heterogeneous surfaces[55] while the Langmuir isotherm model assumes that constant energy of adsorption and independent of the coverage surface where the adsorption occurs on the localized site with no interaction between the adsorbate. Table 6 showed that the values of mean free energy of adsorption, E, from the DR equation for RBV5R dye at the different solution temperature were lesser than 8 kJ/mol. Therefore, the adsorption mechanism in this study is physical in nature.

Adsorption kinetics

Adsorption kinetic remains a vital characteristic that defines the effectiveness of adsorption. The dynamics of adsorption process describe the solutes' adsorption rates which is a function of contact time of dye adsorbed at the solid-solutions interface.[78] The performance of AC can be easily compared by the rate constants of adsorption.[16] Four kinetics models (PFO, PSO, Elovich, and Avrami models) were used to test the adsorption data. The parameters are reported in Table 7. Figure 8 represents the linearized graphs of four kinetic models for RBV5R dye adsorption onto LLAC at 30 °C at various initial concentrations. The fittings of the equilibrium data were done using the linearized forms of Eqs. (14)–(16). The R^2 values obtained from isothermal models were correlated for the fitting of the adsorption data. The closer the R^2 value to 1, the better the fit. Kinetic studies were also investigated for adsorption systems at 45 °C and 60 °C (see Figure S3 in the supporting information). In comparison with other models, PFO kinetics model offered the best fitting (Figure 8) judging from R^2 value which shows a consistent trend (Table 7).[59] The R^2 values are closer to 1 indicating good agreements between $q_{e,exp.}$ and $q_{e.cal}$ values. This means that equilibrium is attained faster at low initial RBV5R dye concentrations than at high concentrations.[60] Elovich model describes the nature of adsorption systems. This finding reported is similar to previous works.[25,39,81] The plot of q_t against *ln(t)* showed a linear relation with (1/b) values reflecting the number of available sites for adsorption while the value of (1/b) ln(ab) indicated the quantities adsorbed.

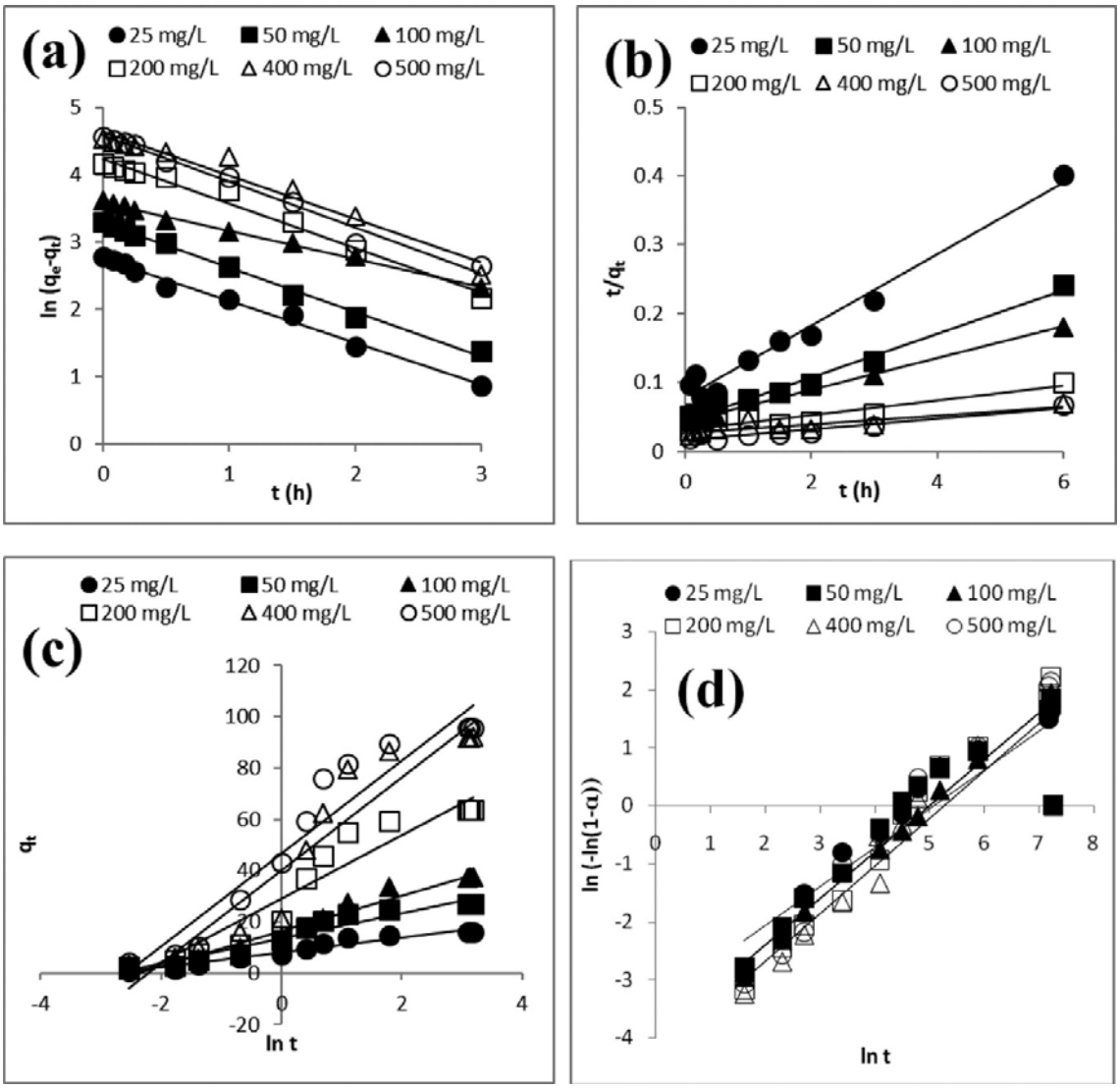

Figure 8. Linearized kinetic model plots of for RBV5R dye adsorption on LLAC at 30 ^{0}C; (a)pseudo-first order, (b) pseudo-second order, (c) Elovich and (d) Avrami.

Table 7. Kinetic model constant parameter for RBV5R adsorption at 30 °C.

Model	Kinetic Parameters	Initial RBV5R dye concentration (mg/L)					
		25	50	100	200	400	500
Pseudo-first-order	Q_e, exp (mg g^{-1})	16.108	26.902	37.367	63.727	91.980	95.700
	K_1 (min^{-1})	0.626	0.656	00418	0.659	0.643	0.681
	$Q_e$cal (mg g^{-1})	15.709	26.369	36.050	68.463	101.738	97.115
	R^2	0.992	0.995	0.994	0.983	0.959	0.980
	Δq_e (%)	2.477	1.981	3.525	7.432	10.609	1.479
Pseudo-second-order	K_2 (min^{-1})	0.0346	0.0224	0.0121	0.0038	0.0017	0.0034
	$Q_e$cal (mg g^{-1})	19.231	31.646	43.478	93.458	153.846	131.579
	R^2	0.976	0.987	0.990	0.909	0.769	0.917
	Δqe (%)	19.388	17.634	16.354	46.654	67.260	37.491
Elovich	α (mg g^{-1} min^{-1})	5.474	3.217	1.570	0.848	0.501	0.725
	β (g mg^{-1})	2.902	4.893	6.911	12.366	18.165	18.116
	R^2	0.950	0.938	0.974	0.921	0.911	0.929
Avrami	k_{AV} (min^{-1})	0.0062	0.0068	0.0052	0.0059	0.0051	0.0067
	n_{AV}	0.669	0.683	0.723	0.813	0.20	0.798
	R^2	0.835	0.843	0.884	0.861	0.867	0.845
	Q_e, exp (mg g^{-1})	16.108	26.902	37.367	63.727	91.980	95.700

Summarily, the kinetic parameters obtained from Figure 8 for adsorption of RBV5R dye onto LLAC at 30 °C are tabulated in Table 7. Also, the PSO model parameters are in good agreement with the experimentally observed values, particularly at low initial concentrations. At high initial concentrations, the PSO model shows deviation from the experimental data showing that adsorption of RBV5R dye onto LLAC did not follow the PSO model. The adsorption system at 45 °C and 60 °C also gave similar plots. These observations are in agreement with other studies.[2,48,50]

Intraparticle diffusion and mechanistic studies

Although several factors control the adsorption rate:[25,39,53,65,82] (i) film diffusion in which adsorbate ion travel toward the adsorbent external surface. (ii) particle diffusion, where adsorbate ion travels within the pores of the adsorbent where less adsorption occurred on the adsorbent's exterior surface. (iii) adsorption of the adsorbate ion on the adsorbent's interior surface.[25] Practically, the adsorption mechanism remains a significant and major factor that governs the adsorption kinetics such that there exists the occurrence of the initial curved portion due to the fast surface adsorption and external diffusion of RBV5R dye unto LLAC.[39]

Figure 9 shows IPD plots at different initial RBV5R dye concentrations onto LLAC at 30 °C resulting in three different phases of RBV5R dye adsorption: the first stage is instantaneous adsorption which is the involvement of strong electrostatic attractions occurring between RBV5R dye and LLAC external surfaces. In this stage, there is a boundary diffusion layer of RBV5R dye molecules. The mass transfer is governed by several relationships: the mechanism of adsorption, liquid-solid phase coupling and initial-to-boundary factors. This further predicts that the attainment of the equilibrium are IPD-controlled.[39] The second phase is attributed to a gradual stage revealing that the IPD is the slowest step. This step is called the rate-determining step.[83,84] Following this was the third phase with the comparatively slower adsorption processes having the linear stability of approaching the equilibrium (plateau) stage; this is called the maximum adsorption stage. This was due to lower concentrations of RBV5R dye remaining in the solution. The values of IPD- model constants; k_t and C were estimated from the q_t (mg/g) vs. $t^{1/2}$ ($h^{1/2}$) plot are reported in Table 8. As shown in Figure 9, it means that the IPD plot was not the only rate-determining mechanism in the process of adsorption. The values of k_{dif}, C, and R^2 for the three stages are reported in Table 8.

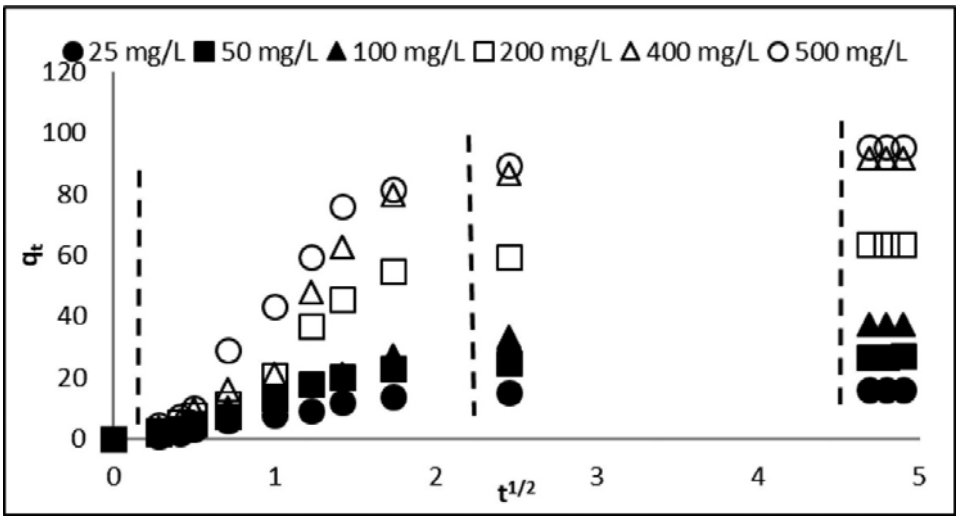

Figure 9. Plot of intraparticle diffusion model for (b) RBV5R dye adsorption on LLAC at 30 ^{0}C.

Table 8. Intraparticle diffusion model constant for RBV5R adsorption onto LLAC at 30 ^{o}C (k, mg/g $h^{1/2}$; initial dye concentration, mg/L).

Initial concentration	k_{p1}	k_{p2}	k_{p3}	C_1	C_2	C_3	$(R_1)^2$	$(R_2)^2$	$(R_3)^2$
25	2.896	6.790	0.465	0	0.464	13.778	1	0.914	0.994
50	5.573	11.645	0.864	0	0.518	22.695	1	0.894	0.999
100	6.641	15.066	1.682	0	1.225	29.23	1	0.979	0.999
200	9.341	30.519	1.757	0	−5.784	55.272	1	0.912	0.997
400	12.516	45.182	2.222	0	−12.10	81.21	1	0.916	0.998
500	15.189	44.317	2.622	0	−2.834	83.1	1	0.889	0.996

From Table 8, the $k_{p1,}$ and k_{p2} values for the three phases increased with an increase in the initial RBV5R dye concentration due to the significant increase of the concentration gradients called the driving force which further enhance the rate of diffusion of RBV5R dye onto LLAC.[25,39,48,50,65,85] The value of C also increases as the initial RBV5R dye concentration increases, which implies that there is an increase in the thickness of the boundary layer.[50,86]

Interestingly, the first phase of adsorption was completed within the first minutes due to the rapid RBV5R dye uptake by LLAC. Then the second phase of IPD control was reached whereas the third phase was reached at high concentration. Adsorption increases very fast in the first phase and later decreases as time increases, implying that the equilibrium was achieved fast. This behavior clarifies the major disparity among k_1, k_2 and k_3. For the second and third stages, the linear plot deviated from origin. The non-linearity of the q_t (mg/g) vs. $t^{1/2}$ $(h^{1/2})$ plot obtained for RBV5R dye adsorption onto LLAC (Figure 9) with deviation from zero reveals that IPD was not the only rate-determining step. The divergence might be as a result of differences in the rate of mass transfer occurring both at the initial and final phases.[87] Plots with the non-zero origin ($C \neq 0$) shows that IPD occurred in the adsorption processes but it is not the only controlling variable for the rate of reaction. The intercept "C" shows proportional relationship with the boundary layer having a noticeable extent of thickness at 30 °C.[39] This further helped to establish the propensity of LLAC to either adsorb RBV5R dye or remain in the solution. The higher values of "C" depicted an enhanced capacity of adsorption.

Another principal characteristic involved in the process of adsorption is the actual slow step; therefore, for the prediction of the actual slow steps, the Boyd model was applied. Figure 10

presents the Boyd model plots for the RBV5R dye uptake onto LLAC. The linearized plots of B_t values versus time for various dye initial concentrations at 30 °C (Figure 10), revealed that the linear plots for all initial RBV5R dye concentration did not pass through the origin, thus confirming that the rate-controlling step in the adsorption processes is determined by external mass transfers.[88] This was because of the extent of difference in the rate of mass transfer between the first and second phases of external mass transfer (film diffusion) where the particles' diffusion was the rate-limiting step. These first and second adsorption phases are ascribed to the macropore and micropore diffusions respectively.[2,64,73,89]

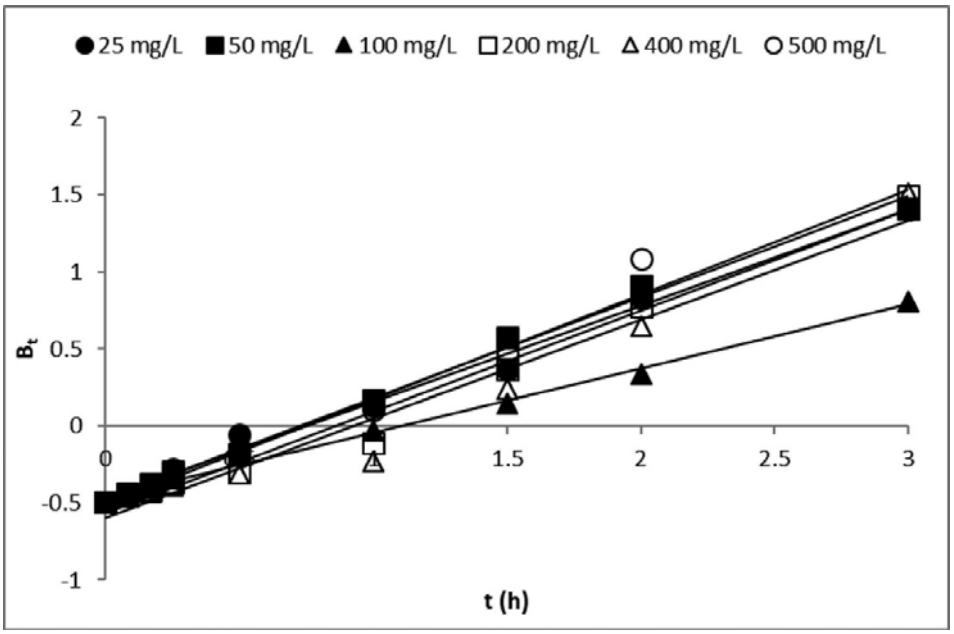

Figure 10. Plot of Boyd model for the adsorption of RBV5R dye on LLAC at 30 ^{0}C.

Thermodynamic studies

Thermodynamic parameters (ΔG^0, ΔH^0 and ΔS^0) remains very important factors in adsorption systems; they are key parameters for the adsorbent sorption capacity.[2,90] These three thermodynamic parameters were considered based on the transferring of 1 mole of solute from the solution onto the interface of the solid-liquid. The values of ΔS^0 and ΔH^0 are intercept and slope obtained from the Van't Hoff plot of ln K_L (L/mg) versus 1/T (Figure 11a). The plot of ln k_2 vs. 1/T gave a linear graph with a slope of -Ea/R giving a positive value of energy of activation (Figure 11b). The minimum energy E_a needed for the reaction to occur was 2.811 kJ/mol, which is less than 40 kJ/mol. This signifies that the rate-controlling step for RBV5R dye adsorption is physically controlled and a rapid process which occurred at low temperature unlike chemical adsorption.[91] The values of ΔG^0, ΔH^0, ΔS^0, and E_a for RBV5R dye adsorption onto LLAC at different temperatures are listed in Table 9. The negative values of ΔG^0 (ranging from −11.122 to −11.936 kJmol^{-1}) obtained for the adsorption of RBV5R dye onto LLAC depict the spontaneity of the adsorption process; with a significant preference for the RBV5R dye onto LLAC.[12,92–93] These results are in agreement with the effects of solution temperature at 45 °C and 60 °C respectively. Increasing the temperature leads to a decrease in the ΔG^0 values which showed a less driving force, resulting in less adsorption.[2,82] The ΔH^0 value was positive (20.160 kJmol^{-1}) revealing an endothermic nature of the adsorption process (Table 9). The positive value of ΔS (27.140 kJmol^{-1}K^{-1}) confirmed the affinity of LLAC for

the RBV5R dye uptake and increased randomness at the solid-solution interface during the adsorption process.

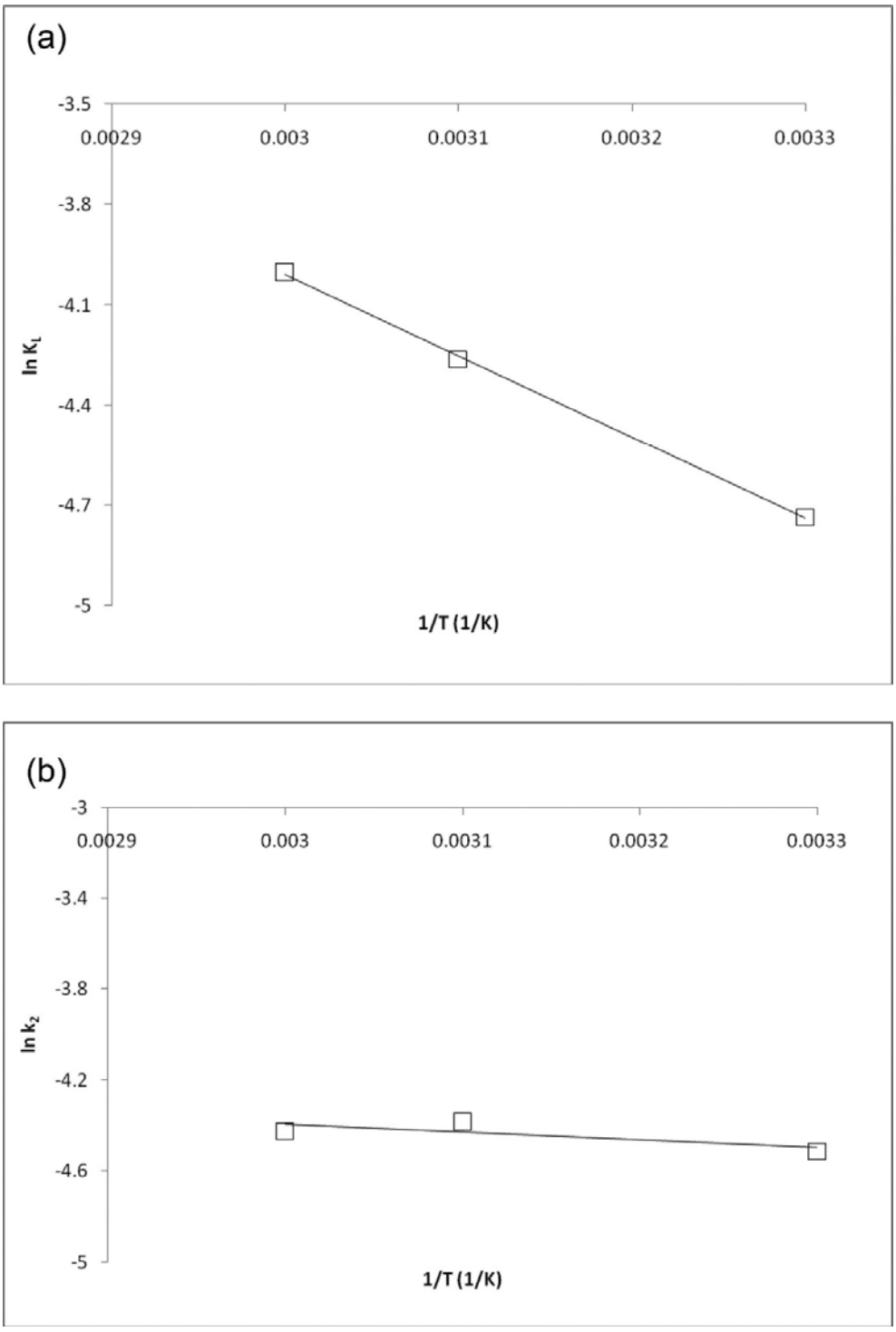

Figure 11. (a) Plots of ln K_L versus 1/T for adsorption of RBV5R dye on the LLAC. (b) Plot of ln k2 versus 1/T for adsorption of RBV5R dye onto LLAC.

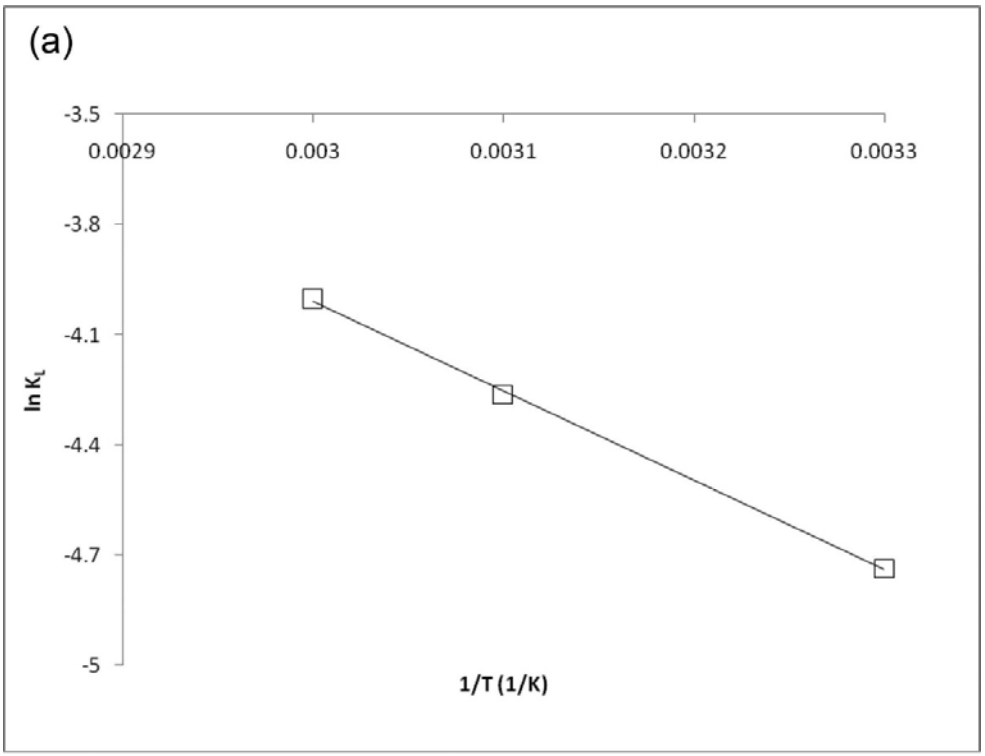

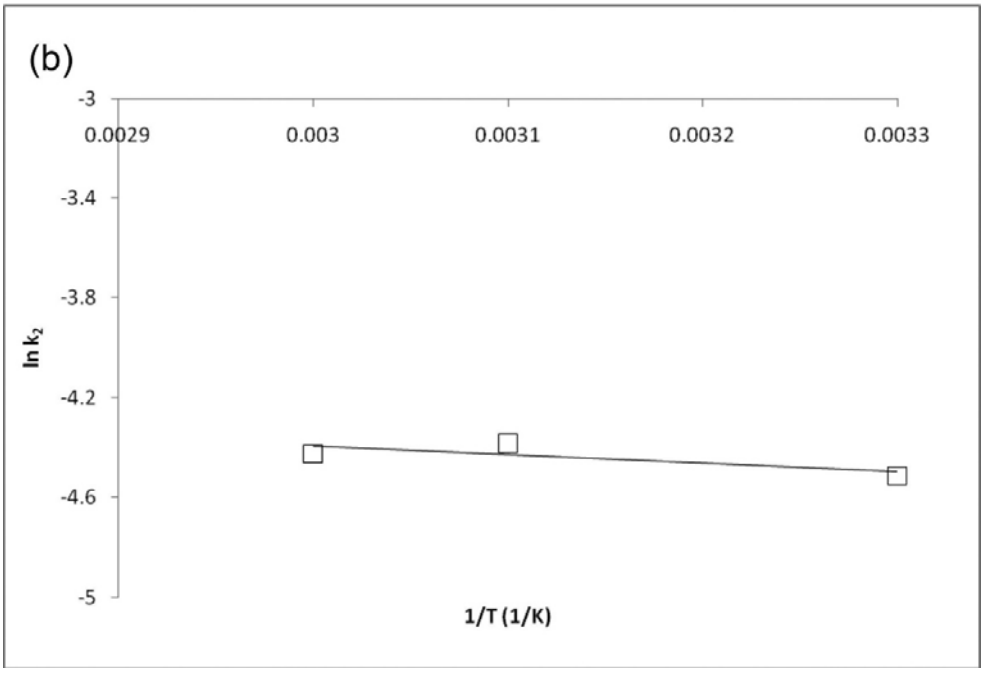

Figure 11 **b**: Plot of ln k_2 versus 1/T for adsorption of RBV5R dye onto LLAC.

Table 9. Thermodynamic parameters for adsorption of RBV5R dyes on LLAC.

				$-\Delta G^{o}$(kJ/mol)		
Dye	ΔH^{o}(kJ/mol)	ΔS^{o}(J/mol.K)	E_a(kJ/mol.K)	303 K	318 K	333 K
RBV5R	20.160	27.140	2.811	11.936	11.529	11.122

Conclusion

Low-cost AC was successfully prepared from Lemon grass leaf for the removal of RBV5R dye using the physicochemical activation techniques. Surface area of 836.04 m^2/g, mesopore surface area of 598.64 m^2/g, total pore volume of 0.472 cm^3/g, and average pore diameter of 3.62 nm of LLAC was obtained. Batch adsorption studies with four different operational variables: initial RBV5R dye concentration (25 mg/L–500 mg/L), contact time (0–24 hrs), solution pH (2–12) and solution temperatures (30–60 °C) revealed that the percentage RBV5R dye removal decreases with increase in initial dye concentration, contact time and solution temperature. RBV5R dye adsorption onto LLAC was best represented by Freundlich and Koble Corrigan isotherm models. The monolayer adsorption capacities (q_m) obtained for Langmuir and Koble Corrigan isotherm models are 125 and 342.9 mg/g respectively. For the adsorption kinetic model, the adsorption RBV5R dye on LLAC fitted PFO kinetic model most with q_{max} of 95.7 mg/g which increased with increase in temperature, signifying an endothermic process of adsorption. The adsorption process was spontaneous, endothermic in nature and physically controlled.

Acknowledgments

Supports obtained from Research University Grant (1001/PJKIMIA/8014061) from Universiti Sains Malaysia (first and second author), LAUTECH 2016 TET Fund Institution Based Research Intervention (TETFUND/DESS/UNI/OGBOMOSO/RP/VOL. IX) given to the corresponding author and the TWAS-NRF for Doctoral scholarship awarded to the third author (UID: 105453 & Reference: SFH160618172220 and UID: 121108 & Reference: MND190603441389) are all acknowledged.

References

1. Adegoke, K. A.; Bello, O. S. Dye Sequestration Using Agricultural Wastes as Adsorbents. *Water Resour. Ind.* 2015, *12*, 8–24. doi:https://doi.org/10.1016/j.wri.2015.09.002.
2. Ahmad, M. A.; Afandi, N. S.; Adegoke, K. A.; Bello, O. S. Optimization and Batch Studies on Adsorption of Malachite Green Dye Using Rambutan Seed Activated Carbon. *Desalin. Water Treat.* 2016, *57*, 21487–21511. doi:https://doi.org/10.1080/19443994.2015.1119744.
3. Adeyemo, A. A.; Adeoye, I. O.; Bello, O. S. Adsorption of Dyes Using Different Types of Clay: A Review. *Appl. Water Sci.* 2017, *7*, 543–568. doi:https://doi.org/10.1007/s13201-015-0322-y.
4. Bulgariu, L.; Escudero, L. B.; Bello, O. S.; Iqbal, M.; Nisar, J.; Adegoke, K. A.; Alakhras, F.; Kornaros, M.; Anastopoulos, I. The Utilization of Leaf-Based Adsorbents for Dyes Removal: A Review. *J. Mol. Liq.* 2019, *276*, 728–747. doi:https://doi.org/10.1016/J.MOLLIQ.2018.12.001.
5. Bello, O. S.; Adegoke, K. A.; Olaniyan, A. A.; Abdulazeez, H. Dye Adsorption Using Biomass Wastes and Natural Adsorbents: overview and Future Prospects. *Desalin. Water Treat.* 2013, *53*, 1–1315. doi:https://doi.org/10.1080/19443994862028.
6. Arslan, I.; Balcioğlu, I. A.; Bahnemann, D. W. Advanced Chemical Oxidation of Reactive Dyes in Simulated Dyehouse Effluents by ferrioxalate-Fenton/UV-a and TiO2/UV-a Processes. *Dye. Pigment* 2000, *47*, 207–218. DOI: https://doi.org/10.1016/S0143-7208(00)00082-6.

7. Rehman, R.; Mahmud, T.; Anwar, J.; Salman, M. Isothermal Modeling of Batch Biosorption of Brilliant Green Dye from Water by Chemically Modified Eugenia jambolana Leaves. *J. Chem. Soc. Pakistan.* 2012, *34*, 136–143. https://www.researchgate.net/publication/232041885.
8. Adegoke, K. A.; Oyewole, R. O.; Lasisi, B. M.; Bello, O. S. Abatement of Organic Pollutants Using Fly Ash Based Adsorbents. *Water Sci. Technol.* 2017, *76*, 2580–2592. DOI: https://doi.org/10.2166/wst.2017.437.
9. Bello, I. A.; Bello, O. S.; Adegoke, K. A. Effects of Modifying Agents on the Dyeability of Cotton Fabric Using Malachite Green Dye. *Ann. Sci. Technol.* 2017, *2*, 26–36. doi:https://doi.org/10.2478/ast-2018-0005.
10. Bello, O. S.; Ahmad, M. A. Removal of Remazol Brilliant Violet-5R Dye Using Periwinkle Shells. *Chem. Ecol.* 2011, *27*, 481–492. doi:https://doi.org/10.1080/02757540.2011.600696.
11. Ahmad, M. A.; Ahmad, N.; Bello, O. S. Adsorptive Removal of Malachite Green Dye Using Durian Seed-Based Activated Carbon. *Water. Air. Soil Pollut* 2014, *225*, 2057–2076. DOI: https://doi.org/10.1007/s11270-014-2057-z.
12. Bello, O. S.; Ahmad, M. A. Adsorptive Removal of a Synthetic Textile Dye Using Cocoa Pod Husks. *Toxicol. Environ. Chem.* 2011, *93*, 1298–1308. doi:https://doi.org/10.1080/02772248.2011.590490.
13. Wang, Y.; Zhao, L.; Hou, J.; Peng, H.; Wu, J.; Liu, Z.; Guo, X. Kinetic, Isotherm, and Thermodynamic Studies of the Adsorption of Dyes from Aqueous Solution by Cellulose-Based Adsorbents. *Water Sci. Technol.* 2018, *77*, 2699–2708. DOI: https://doi.org/10.2166/wst.2018.229.
14. Amel, K.; Hassen, M. A.; Kerroum, D. Isotherm and Kinetics Study of Biosorption of Cationic Dye onto Banana Peel, in. *Energy Procedia* 2012, *19*, 286–295. doi:https://doi.org/10.1016/j.egypro.2012.05.208.
15. Thambiraj, S.; Sharmila, G.; Ravi Shankaran, D. Green Adsorbents from Solid Wastes for Water Purification Application. *Mater. Today Proc.* 2018, *5*, 16675–16683. doi:https://doi.org/10.1016/j.matpr.2018.06.029.
16. Demirbas, A. Agricultural Based Activated Carbons for the Removal of Dyes from Aqueous Solutions: A Review. J. Hazard. Mater. 2009, *167*, 1–9. DOI: https://doi.org/10.1016/j.jhazmat.2008.12.114.
17. Yagub, M. T.; Sen, T. K.; Afroze, S.; Ang, H. M. Dye and Its Removal from Aqueous Solution by Adsorption: A Review. *Adv. Colloid Interface Sci.* 2014, *209*, 172–184. DOI: https://doi.org/10.1016/j.cis.2014.04.002.
18. De Gisi, S.; Lofrano, G.; Grassi, M.; Notarnicola, M. Characteristics and Adsorption Capacities of Low-Cost Sorbents for Wastewater Treatment: A Review. *Sustain. Mater. Technol.* 2016, *9*, 10–40. doi:https://doi.org/10.1016/j.susmat.2016.06.002.
19. Thirumavalavan, M.; Lai, Y. L.; Lin, L. C.; Lee, J. F. Cellulose-Based Native and Surface Modified Fruit Peels for the Adsorption of Heavy Metal Ions from Aqueous Solution: Langmuir Adsorption Isotherms. *J. Chem. Eng. Data* 2010, *55*, 1186–1192. doi:https://doi.org/10.1021/je900585t.
20. Singh, H.; Chauhan, G.; Jain, A. K.; Sharma, S. K. Adsorptive Potential of Agricultural Wastes for Removal of Dyes from Aqueous Solutions. *J. Environ. Chem. Eng.* 2017, *5*, 122–135. doi:https://doi.org/10.1016/j.jece.2016.11.030.
21. Jain, S. N.; Gogate, P. R. NaOH-Treated Dead Leaves of Ficus Racemosa as an Efficient Biosorbent for Acid Blue 25 Removal. *Int. J. Environ. Sci. Technol.* 2017, *14*, 531–542. doi:https://doi.org/10.1007/s13762-016-1160-7.

22. Atoyebi, O. M.; Bello, O. S. Indian Spinach Leaf Powder as Adsorbent for Malachite Green Dye Removal from Aqueous Solution. *Covenant J. Phys. Life Sci.* 2014, *2*, 54–67.
23. Wong, S.; Ngadi, N.; Inuwa, I. M.; Hassan, O.; Wang, P.; Ma, Q.; Hu, D.; Wang, L.; Imam, S. S.; Panneerselvam, P.; et al. Application of Peanut Shell as a Low-Cost Adsorbent for the Removal of Anionic Dye from Aqueous Solutions. *J. Clean. Prod.* 2012, *8*, 5–7., DOI: https://doi.org/10.1089/ees.2010.0385.
24. Jain, S. N.; Gogate, P. R. Adsorptive Removal of Acid Violet 17 Dye from Wastewater Using Biosorbent Obtained from NaOH and H2SO4 Activation of Fallen Leaves of Ficus Racemosa. *J. Mol. Liq.* 2017, *243*, 132–143. doi:https://doi.org/10.1016/j.molliq.2017.08.009.
25. Ojedokun, A. T.; Bello, O. S. Kinetic Modeling of Liquid-Phase Adsorption of Congo Red Dye Using Guava Leaf-Based Activated Carbon. *Appl. Water Sci.* 2017, *7*, 1965–1977. doi:https://doi.org/10.1007/s13201-015-0375-y.
26. Tang, Y.; Li, Y.; Zhao, Y.; Zhou, Q.; Peng, Y. Enhanced Removal of Methyl Violet Using NaOH-Modified *C. camphora* Leaves Powder and Its Renewable Adsorption. *DWT* 2017, *98*, 306–314. doi:https://doi.org/10.5004/dwt.2017.21569.
27. Gunasekar, V.; Ponnusami, V. Kinetics, Equilibrium, and Thermodynamic Studies on Adsorption of Methylene Blue by Carbonized Plant Leaf Powder. *J. Chem.* 2013, *2013*, 1–6. doi:https://doi.org/10.1155/2013/415280.
28. Hameed, B. H.; Din, A. T. M.; Ahmad, A. L. Adsorption of Methylene Blue onto Bamboo-Based Activated Carbon: Kinetics and Equilibrium Studies. J. Hazard. Mater. 2007, *141*, 819–825. DOI: https://doi.org/10.1016/j.jhazmat.2006.07.049.
29. Ghosh, S. K.; Bandyopadhyay, A. Adsorption of Methylene Blue onto Citric Acid Treated Carbonized Bamboo Leaves Powder: Equilibrium, Kinetics, Thermodynamics Analyses. *J. Mol. Liq.* 2017, *248*, 413–424. doi:https://doi.org/10.1016/j.molliq.2017.10.086.
30. Yang, J. X.; Hong, G. B. Adsorption Behavior of Modified Glossogyne Tenuifolia Leaves as a Potential Biosorbent for the Removal of Dyes. *J. Mol. Liq.* 2018, *252*, 289–295. doi:https://doi.org/10.1016/j.molliq.2017.12.142.
31. Bello, O. S.; Owojuyigbe, E. S.; Babatunde, M. A.; Folaranmi, F. E. Sustainable Conversion of Agro-Wastes into Useful Adsorbents. *Appl. Water Sci.* 2017, *7*, 3561–3571. doi:https://doi.org/10.1007/s13201-016-0494-0.
32. Cabal, B.; Budinova, T.; Ania, C. O.; Tsyntsarski, B.; Parra, J. B.; Petrova, B. Adsorption of Naphthalene from Aqueous Solution on Activated Carbons Obtained from Bean Pods. J. Hazard. Mater. 2009, *161*, 1150–1156. DOI: https://doi.org/10.1016/j.jhazmat.2008.04.108.
33. Cazetta, A. L.; Vargas, A. M. M.; Nogami, E. M.; Kunita, M. H.; Guilherme, M. R.; Martins, A. C.; Silva, T. L.; Moraes, J. C. G.; Almeida, V. C. NaOH-Activated Carbon of High Surface Area Produced from Coconut Shell: Kinetics and Equilibrium Studies from the Methylene Blue Adsorption. *Chem. Eng. J.* 2011, *174*, 117–125. doi:https://doi.org/10.1016/j.cej.2011.08.058.
34. Rashid, R. A.; Jawad, A. H.; Ishak, M. A. B. M.; Kasim, N. N. FeCl 3 -Activated Carbon Developed from Coconut Leaves: Characterization and Application for Methylene Blue Removal. *JSM* 2018, *47*, 603–610. doi:https://doi.org/10.17576/jsm-2018-4703-22.
35. Jain, S. N.; Gogate, P. R. Acid Blue 113 Removal from Aqueous Solution Using Novel Biosorbent Based on NaOH Treated and Surfactant Modified Fallen Leaves of Prunus Dulcis. *J. Environ. Chem. Eng.* 2017, *5*, 3384–3394. doi:https://doi.org/10.1016/j.jece.2017.06.047.

36. Gong, L.; Sun, W.; Kong, L. Adsorption of Methylene Blue by NaOH-Modified Dead Leaves of Plane Trees. *CWEEE* 2013, *02*, 13–19. doi:https://doi.org/10.4236/cweee.2013.22b003.
37. Hussin, Z. M.; Talib, N.; Hussin, N. M.; Hanafiah, M. A. K. M.; Khalir, W. K. A. W. M. Methylene Blue Adsorption onto NaOH Modified Durian Leaf Powder: Isotherm and Kinetic Studies. *Am. J. Environ. Eng.* 2015, *5*, 38–43. DOI: https://doi.org/10.5923/c.ajee.201501.07.
38. Bello, O. S.; Adegoke, K. A.; Akinyunni, O. O. Preparation and Characterization of a Novel Adsorbent from Moringa Oleifera Leaf. *Appl. Water Sci.* 2017, *7*, 1295–1305. doi:https://doi.org/10.1007/s13201-015-0345-4.
39. Bello, O. S.; Lasisi, B. M.; Adigun, O. J.; Ephraim, V. Scavenging Rhodamine B Dye Using Moringa Oleifera Seed Pod. *Chem. Speciat. Bioavailab.* 2017, *29*, 120–134. doi:https://doi.org/10.1080/09542299.2017.1356694.
40. Ahmaruzzaman, M.; Ahmed, M. J. K.; Begum, S. Remediation of Eriochrome Black T-Contaminated Aqueous Solutions Utilizing H3PO4 -Modified Berry Leaves as a Non-Conventional Adsorbent. *Desalin. Water Treat.* 2015, *56*, 1507–1519. doi:https://doi.org/10.1080/19443994.2014.950995.
41. Bello, O. S.; Adegoke, K. A.; Sarumi, O. O.; Lameed, O. S. Functionalized Locust Bean Pod (*Parkia biglobosa*) Activated Carbon for Rhodamine B Dye Removal. *Heliyon* 2019, *5*, e02323 DOI: https://doi.org/10.1016/j.heliyon.2019.e02323.
42. Ahn, D. H.; Chang, W. S.; Il Yoon, T. Dyestuff Wastewater Treatment Using Chemical Oxidation, Physical Adsorption and Fixed Bed Biofilm Process. *Process Biochem.* 1999, *34*, 429–439. DOI: https://doi.org/10.1016/S0032-9592(98)00111-3.
43. Deveci, T.; Unyayar, A.; Mazmanci, M. A. Production of Remazol Brilliant Blue R Decolourising Oxygenase from the Culture Filtrate of Funalia Trogii ATCC. *J. Mol. Catal. B Enzym.* 2004, *30*, 25–32. DOI: https://doi.org/10.1016/j.molcatb.2004.03.002.
44. Ahmad, M. A.; Ahmad Puad, N. A.; Bello, O. S. Kinetic, Equilibrium and Thermodynamic Studies of Synthetic Dye Removal Using Pomegranate Peel Activated Carbon Prepared by Microwave-Induced KOH Activation. *Water Resour. Ind.* 2014, *6*, 18–35. DOI: https://doi.org/10.1016/j.wri.2014.06.002.
45. Bello, O. S.; Ahmad, M. A.; Ahmad, N. Adsorptive Features of Banana (*Musa paradisiaca*) Stalk-Based Activated Carbon for Malachite Green Dye Removal. *Chem. Ecol.* 2012, *28*, 153–167. doi:https://doi.org/10.1080/02757540.2011.628318.
46. Eichlerová, I.; Homolka, L.; Benada, O.; Kofroňová, O.; Hubálek, T.; Nerud, F. Decolorization of Orange G and Remazol Brilliant Blue R by the White Rot Fungus Dichomitus Squalens: Toxicological Evaluation and Morphological Study. *Chemosphere* 2007, *69*, 795–802. doi:https://doi.org/10.1016/j.chemosphere.2007.04.083.
47. Giannakoudakis, D. A.; Hosseini-Bandegharaei, A.; Tsafrakidou, P.; Triantafyllidis, K. S.; Kornaros, M.; Anastopoulos, I. Aloe Vera Waste biomass-based adsorbents for the removal of aquatic pollutants: A review . J. Environ. Manage. 2018, *227*, 354–364. DOI: https://doi.org/10.1016/j.jenvman.2018.08.064.
48. Ahmad, M. A.; Ahmad, N.; Bello, O. S. Modified Durian Seed as Adsorbent for the Removal of Methyl Red Dye from Aqueous Solutions. *Appl. Water Sci.* 2015, *5*, 407–423. doi:https://doi.org/10.1007/s13201-014-0208-4.
49. Ahmad, M. A.; Ahmed, N. B.; Adegoke, K. A.; Bello, O. S. Sorption Studies of Methyl Red Dye Removal Using Lemon Grass (*Cymbopogon citratus*). *Chem. Data Collect* 2019, *22*, 100249. doi:https://doi.org/10.1016/j.cdc.2019.100249.
50. Ahmad, M. A.; Alrozi, R. Removal of Malachite Green Dye from Aqueous Solution Using Rambutan Peel-Based Activated Carbon: Equilibrium, Kinetic and

Thermodynamic Studies. *Chem. Eng. J.* 2011, *171*, 510–516. doi:https://doi.org/10.1016/j.cej.2011.04.018.
51. Bello, O. S.; Banjo, S. Equilibrium, Kinetic, and Quantum Chemical Studies on the Adsorption of Congo Red Using Imperata Cylindrica Leaf Powder Activated Carbon. *Toxicol. Environ. Chem.* 2012, *94*, 1114–1124. doi:https://doi.org/10.1080/02772248.2012.691504.
52. Inyinbor, A. A.; Adekola, F. A.; Olatunji, G. A. Kinetics, Isotherms and Thermodynamic Modeling of Liquid Phase Adsorption of Rhodamine B Dye onto Raphia Hookerie Fruit Epicarp. *Water Resour. Ind.* 2016, *15*, 14–27. doi:https://doi.org/10.1016/j.wri.2016.06.001.
53. Olakunle, M. O.; Inyinbor, A. A.; Dada, A. O.; Bello, O. S. Combating Dye Pollution Using Cocoa Pod Husks: A Sustainable Approach. *Int. J. Sustain. Eng.* 2018, *11*, 4–15. doi:https://doi.org/10.1080/19397038.2017.1393023.
54. Cassady, J. C.; Johnson, R. E. Cognitive Test Anxiety and Academic Performance. *Contemp. Educ. Psychol.* 2002, *27*, 270–295. doi:https://doi.org/10.1006/ceps.2001.1094.
55. Prusky, G. T.; West, P. W. R.; Douglas, R. M. Reduced Visual Acuity Impairs Place but Not Cued Learning in the Morris Water Task. *Behav. Brain Res.* 2000, *116*, 135–140. doi:https://doi.org/10.1016/S0166-4328(00)00267-9.
56. Zheng, H.; Liu, D.; Zheng, Y.; Liang, S.; Liu, Z. Sorption Isotherm and Kinetic Modeling of Aniline on Cr-Bentonite. J. Hazard. Mater. 2009, *167*, 141–147. DOI: https://doi.org/10.1016/j.jhazmat.2008.12.093.
57. Dubinin, M. M. The Potential Theory of Adsorption of Gases and Vapors for Adsorbents with Energetically Nonuniform Surfaces. *Chem. Rev.* 1960, *60*, 235–241. doi:https://doi.org/10.1021/cr60204a006.
58. Ajemba, R. O. Adsorption of Malachite Green from Aqueous Solution Using Activated Ntezi Clay:Optimization. *Isotherm Kinetic Stud.* 2014, *27*, 839–854. DOI: https://doi.org/10.5829/idosi.ije.2014.27.06c.03.
59. Lindgreen, A.; Lindgreen, A. Corruption and Unethical Behavior: Report on a Set of Danish Guidelines. *J. Bus. Ethics* 2004, *51*, 31–39. doi:https://doi.org/10.1023/B:BUSI.0000032388.68389.60.
60. Ho, Y. S.; McKay, G. Pseudo-Second Order Model for Sorption Processes. *Process Biochem.* 1999, *34*, 451–465. doi:https://doi.org/10.1016/S0032-9592(98)00112-5.
61. Aharoni, C.; Ungarish, M. Kinetics of Activated Chemisorption. Part 2. - Theoretical Models. *J. Chem. Soc., Faraday Trans. 1*. 1977, *73*, 456–464. doi:https://doi.org/10.1039/F19777300456.
62. Ungarish, M.; Aharoni, C. Kinetics of Chemisorption. Deducing Kinetic Laws from Experimental Data. *J. Chem. Soc., Faraday Trans. 1* 1981, *77*, 975–985. doi:https://doi.org/10.1039/F19817700975.
63. Di Chiara, G.; Imperato, A. Drugs Abused by Humans Preferentially Increase Synaptic Dopamine Concentrations in the Mesolimbic System of Freely Moving Rats. *Proc. Natl. Acad. Sci. U S A* 1988, *85*, 5274–5278. DOI: https://doi.org/10.1073/pnas.85.14.5274.
64. Khasri, A.; Bello, O. S.; Ahmad, M. A. Mesoporous Activated Carbon from Pentace Species Sawdust via Microwave-Induced KOH Activation: optimization and Methylene Blue Adsorption. *Res. Chem. Intermed.* 2018, *44*, 5737–5757. doi:https://doi.org/10.1007/s11164-018-3452-7.
65. Ojo, T. A.; Ojedokun, A. T.; Bello, O. S. Functionalization of Powdered Walnut Shell with Orthophosphoric Acid for Congo Red Dye Removal. *Part. Sci. Technol.* 2019, *37*, 74–85. doi:https://doi.org/10.1080/02726351.2017.1340914.

66. Bello, O. S.; Siang, T. T.; Ahmad, M. A. Adsorption of Remazol Brilliant Violet-5R Reactive Dye from Aqueous Solution by Cocoa Pod Husk-Based Activated Carbon: Kinetic, Equilibrium and Thermodynamic Studies. *Asia-Pac. J. Chem. Eng.* 2012, *7*, 378–388. doi:https://doi.org/10.1002/apj.557.
67. Ekpete, M. J. N. R.; Horsfall, O. A. Preparation and Characterization of Activated Carbon Derived from Fluted Pumpkin Stem Waste (Telfairia Occidentalis Hook F). *Res. J. Chem. Sci.* 2011, *1*, 10–17. DOI: https://doi.org/10.1688/1862-0000_ZfP_2009_02_Hormuth.
68. Hameed, B. H.; Daud, F. B. M. Adsorption Studies of Basic Dye on Activated Carbon Derived from Agricultural Waste: Hevea Brasiliensis Seed Coat. *Chem. Eng. J.* 2008, *139*, 48–55. doi:https://doi.org/10.1016/j.cej.2007.07.089.
69. N. A.; Rahmat, A. A.; Ali, Salmiati, N.; Hussain, M. S.; Muhamad, R. A.; Kristanti, T. Hadibarata, Removal of Remazol Brilliant Blue R from Aqueous Solution by Adsorption Using Pineapple Leaf Powder and Lime Peel Powder. *Water. Air. Soil Pollut.* 2016, *227*, 1–11. DOI: https://doi.org/10.1007/s11270-016-2807-1.
70. Bello, O. S.; Ahmad, M. A. Preparation and Characterization of Activated Carbon Derived from Rubber Seed Coat. *Chemistry (Easton)* 2012, *21*, 389–395.
71. Tan, I. A. W.; Ahmad, A. L.; Hameed, B. H. Adsorption of Basic Dye on High-Surface-Area Activated Carbon Prepared from Coconut Husk: Equilibrium, Kinetic and Thermodynamic Studies. J. Hazard. Mater. 2008, *154*, 337–346. DOI: https://doi.org/10.1016/j.jhazmat.2007.10.031.
72. Senthilkumaar, S.; Varadarajan, P. R.; Porkodi, K.; Subbhuraam, C. V. Adsorption of Methylene Blue onto Jute Fiber Carbon: Kinetics and Equilibrium Studies. *J. Colloid Interface Sci.* 2005, *284*, 78–82. DOI: https://doi.org/10.1016/j.jcis.2004.09.027.
73. Ahmad, M. A.; Herawan, S. G.; Yusof, A. A. Adsorption Studies of Remazol Brilliant Blue R Dye on Activated Carbon Prepared from Corncob. *Am. J. Mod. Chem. Eng.* 2014, *2014*, 1–12.
74. Ozturk, G.; Silah, H. Adsorptive Removal of Remazol Brilliant Blue R from Water by Using a Macroporous Polystyrene Resin: Isotherm and Kinetic Studies. *Environ. Process* 2020, *7*, 479–492.). doi:https://doi.org/10.1007/s40710-020-00429-4.
75. Putri, K. N. A.; Keereerak, A.; Chinpa, W. Novel Cellulose-Based Biosorbent from Lemongrass Leaf Combined with Cellulose Acetate for Adsorption of Crystal Violet. *Int. J. Biol. Macromol.* 2020, *156*, 762–772. DOI: https://doi.org/10.1016/j.ijbiomac.2020.04.100.
76. Singh, H.; Dawa, T. B. Removal of Methylene Blue Using Lemon Grass Ash as an Adsorbent. *Carbon Lett.* 2014, *15*, 105–112. doi:https://doi.org/10.5714/CL.2014.15.2.105.
77. Saputra, O. A.; Rachma, A. H.; Handayani, D. S. Adsorption of Remazol Brilliant Blue R Using Amino-Functionalized Organosilane in Aqueous Solution. *Indones. J. Chem.* 2017, *17*, 343. doi:https://doi.org/10.22146/ijc.25097.
78. Demirbas, E.; Nas, M. Z. Batch Kinetic and Equilibrium Studies of Adsorption of Reactive Blue 21 by Fly Ash and Sepiolite. *Desalination* 2009, *243*, 8–21. doi:https://doi.org/10.1016/j.desal.2008.04.011.
79. Hadi, M.; Samarghandi, M. R.; McKay, G. Equilibrium Two-Parameter Isotherms of Acid Dyes Sorption by Activated Carbons: Study of Residual Errors. *Chem. Eng. J.* 2010, *160*, 408–416. DOI: https://doi.org/10.1016/j.cej.2010.03.016.
80. Vieth, W. R.; Sladek, K. J. A Model for Diffusion in a Glassy Polymer. *J. Colloid Sci* 1965, *20*, 1014–1033. DOI: https://doi.org/10.1016/0095-8522(65)90071-1.

81. Banat, F.; Al-Asheh, S.; Al-Ahmad, R.; Bni-Khalid, F. Bench-Scale and Packed Bed Sorption of Methylene Blue Using Treated Olive Pomace and Charcoal. Bioresour. Technol. 2007, *98*, 3017–3025. DOI: https://doi.org/10.1016/j.biortech.2006.10.023.
82. Gerçel, O.; Gerçel, H. F.; Koparal, A. S.; Oğütveren, U. B. Removal of Disperse Dye from Aqueous Solution by Novel Adsorbent Prepared from Biomass Plant Material. J. Hazard. Mater. 2008, *160*, 668–674. DOI: https://doi.org/10.1016/j.jhazmat.2008.03.039.
83. Bello, O. S.; Atoyebi, O. M.; Adegoke, K. A.; Fehintola, E. O.; Ojo, A. O. Removal of Toxicant Chromium (VI) from Aqueous Solution Using Different Adsorbents. *J. Chem. Soc. Pakistan* 2015, *37*, 190–206.
84. Hameed, B. H.; Tan, I. A. W.; Ahmad, A. L. Adsorption Isotherm, Kinetic Modeling and Mechanism of 2,4,6-Trichlorophenol on Coconut Husk-Based Activated Carbon. *Chem. Eng. J.* 2008, *144*, 235–244. doi:https://doi.org/10.1016/j.cej.2008.01.028.
85. Nuithitikul, K.; Srikhun, S.; Hirunpraditkoon, S. Kinetics and Equilibrium Adsorption of Basic Green 4 Dye on Activated Carbon Derived from Durian Peel: Effects of Pyrolysis and Post-Treatment Conditions. *J. Taiwan Inst. Chem. Eng.* 2010, *41*, 591–598. DOI: https://doi.org/10.1016/j.jtice.2010.01.007..
86. Khaled, A.; Nemr, A. E.; El-Sikaily, A.; Abdelwahab, O. Removal of Direct N Blue-106 from Artificial Textile Dye Effluent Using Activated Carbon from Orange Peel: Adsorption Isotherm and Kinetic Studies. *J. Hazard. Mater.* 2009, *165*, 100–110. DOI: https://doi.org/10.1016/j.jhazmat.2008.09.122.
87. Mohanty, K.; Naidu, J. T.; Meikap, B. C.; Biswas, M. N. Removal of Crystal Violet from Wastewater by Activated Carbons Prepared from Rice Husk. *Ind. Eng. Chem. Res.* 2006, *45*, 5165–5171. doi:https://doi.org/10.1021/ie060257r.
88. Acharya, J.; Sahu, J. N.; Sahoo, B. K.; Mohanty, C. R.; Meikap, B. C. Removal of Chromium(VI) from Wastewater by Activated Carbon Developed from Tamarind Wood Activated with Zinc Chloride. *Chem. Eng. J.* 2009, *150*, 25–39. DOI: https://doi.org/10.1016/j.cej.2008.11.035.
89. Mopoung, S.; Moonsri, P.; Palas, W.; Khumpai, S. Characterization and Properties of Activated Carbon Prepared from Tamarind Seeds by KOH Activation for Fe(III) Adsorption from Aqueous Solution. *Sci. World J.* 2015, *2015*, 1–9. doi:https://doi.org/10.1155/2015/415961.
90. Bello, O. S.; Auta, M.; Ayodele, O. B. Ackee Apple (Blighia Sapida) Seeds: A Novel Adsorbent for the Removal of Congo Red Dye from Aqueous Solutions. *Chem. Ecol.* 2013, *29*, 58–71. doi:https://doi.org/10.1080/02757540.2012.686606.
91. Ahmad, M. A.; Alrozi, R. Optimization of Rambutan Peel Based Activated Carbon Preparation Conditions for Remazol Brilliant Blue R Removal. *Chem. Eng. J.* 2011, *168*, 280–285. doi:https://doi.org/10.1016/j.cej.2011.01.005.
92. Ahmad, A. A.; Hameed, B. H.; Ahmad, A. L. Removal of Disperse Dye from Aqueous Solution Using Waste-Derived Activated Carbon: Optimization Study. J. Hazard. Mater. 2009, *170*, 612–619. DOI: https://doi.org/10.1016/j.jhazmat.2009.05.021.
93. Ahmad, M. A.; Eusoff, M. A.; Oladoye, P. O.; Adegoke, K. A.; Bello, O. S. Statistical Optimization of Remazol Brilliant Blue R Dye Adsorption onto Activated Carbon Prepared from Pomegranate Fruit Peel. *Chem. Data Collect* 2020, *28*, 1–15. DOI: https://doi.org/10.1016/j.cdc.2020.100426.